Chapter 14 in: Low Temperature Materials and Mechanisms,
Ed. Y. Bar-Cohen, CRC Press (2017)

Chapter 14: Low temperature materials and mechanisms - Applications and challenges*

Ray Radebaugh
NIST Fellow Emeritus
Material Measurement Laboratory
National Institute of Standards and Technology, Boulder, Colorado
Email: radebaugh@boulder.nist.gov. Phone: 303-497-3710, http://cryogenics.nist.gov

and

Yoseph Bar-Cohen
Jet Propulsion Laboratory/Caltech
4800 Oak Grove Drive, M/S 67-119, Pasadena, CA 91109, USA
Phone: 818-354-2610, e-mail: yosi@jpl.nasa.gov Web: http://ndeaa.jpl.nasa.gov

15.1 Introduction

Civilizations have used temperatures near 0 °C for thousands of years. The ability to reach significantly lower temperatures and into the cryogenic range has only become feasible in the last two centuries with the development of effective coolers as described in Chapters 1 and 6. Specifically, the use of cryogenic temperatures offers numerous benefits as listed in **Table 1**. Applications of cryogenics make use of one or more of these benefits. In some cases, the benefits are so profound that the use of an ambient temperature solution is completely impractical. One important example is the use of superconducting magnets for magnetic resonance imaging (MRI). Magnetic fields of 1.5 T are required for obtaining a reasonable resolution. The use of copper electromagnets to produce such fields at room temperature over the volume of a human body would require megawatts of power to overcome the resistive loss in the wire and a massive stream of water to provide the necessary cooling to remove the heat generated from Joule heating.

Table 1: Benefits of Cryogenic Temperatures.

1. Preservation of biological material and food
2. High fluid densities (liquefaction and separation of gases)
3. Macroscopic quantum phenomena (superconductivity and superfluidity)
4. Reduced thermal noise
5. Low vapor pressures (cryopumping)
6. Temporary or permanent property changes
7. Tissue destruction (cryoablation)

However, the production of cryogenic temperatures presents several challenges or disadvantages. Thermodynamic laws, which dictate an increased power input, cannot be overcome, but mechanisms for producing the low temperatures can continually be improved through the use of innovation and motivation. For any application to be useful or marketable, the benefits must outweigh the disadvantages. Typical disadvantages are such things as inconvenience, low reliability, high input power, capital and operating costs, size and weight, vibration, noise, electromagnetic interference (EMI), and heat rejection. The relative importance of these disadvantages depends on the application. In general the disadvantage becomes serious if it dominates the behavior of the complete system. For example, if the reliability of the entire system is limited by the cryocooler, that can be a serious problem and hamper the marketability of the system. If cost of a cryocooler is small compared with the entire system, then cost of the cryocooler no longer becomes a disadvantage. For space applications, the cost of a cryocooler may be rather high to ensure high reliability, but system costs are also usually rather high. For some space applications, mechanisms must be designed to operate at cryogenic temperatures even though there may not be an advantage to doing so. An example of this would be the exploration of distant bodies in the solar system that are extremely cold.

Another challenge to the use of cryogenics involves the proper selection of materials for systems or mechanisms operating at these temperatures or that often span temperatures between the low temperature and ambient temperature. Part of the difficulty is finding data on material properties at cryogenic temperatures. In some cases, data may exist over a different temperature range than what is needed, and some theoretical guidance is thus needed to extrapolate the data to the desired temperature range. This chapter gives examples for applications of cryogenics that make use of each of the seven benefits discussed above. The chapter then goes on to discuss the challenges facing researchers in cryogenics to minimize the disadvantages of operating at cryogenic temperatures with the ultimate goal of making the cryogenic operation invisible to the end user.

15.2 Benefits of Cryogenics

Processes and material properties are strongly affected by temperature, probably more so than by any other physical parameter, including pressure, magnetic field, electric field, etc. Some properties, such as electrical conductivity and thermal conductivity can change by several orders of magnitude when cooled from room temperature to 4 K or below. Most quantum effects occur only at cryogenic temperatures, whereas most metals liquefy only at high temperatures. The ability to harness and apply temperature effects is a unique feature of mankind, and it has contributed to great advances in our civilization. Mankind has discovered abundant benefits and uses for high temperatures, beginning in prehistoric times with the use of fire for warmth, light, and cooking. Later, but still more than 20 centuries ago, mankind learned to forge tools and make crude pottery using heat from fires. As civilization advanced and higher temperatures could be achieved, stronger metals, such as iron, could be forged into tools, and much stronger pottery and china could be produced by the higher temperature firing (sintering) of clay. The industrial revolution ushered in the steam engine and the ability to generate tremendous power for efficient manufacturing and transportation. The enhancement of chemical reactions at higher temperatures has been exploited for the production of vast amounts of new and improved materials in the last century or so [Bar-Cohen, 2014].

High temperature applications began rather early in the history of civilization due to the ease of producing increasingly hotter fires. In contrast, mankind's use of low temperatures has lagged behind that of high temperatures due to the increased difficulty in producing low temperatures. Low temperature applications were limited for many centuries to the use of naturally occurring ice. The practice of using natural ice to treat injuries and inflammation was carried out by Egyptians as early as 2500 BC [Freiman & Bouganim 2005], and Chinese began to use crushed ice in food around 2000 BC. Although ice was first created artificially in the laboratory in 1755, it was not until near the mid-1800s with the development of the steam engine and practical compressors in the industrial revolution that artificial ice could be produced in sufficient quantities to replace natural ice cut from lakes. Until then the sole use of low temperatures was with natural ice for food preservation and a few medical procedures.

Around the mid-1800s the science of thermodynamics was being developed with an understanding of how to produce lower and lower temperatures through the liquefaction of the permanent gases, such as oxygen, nitrogen, hydrogen, and helium. Researchers learned that these gases could be liquefied in a cascade scheme by compression and expansion of each gas. The initial impetus for achieving lower temperatures was for the most part purely scientific. But entrepreneurs soon recognized the benefits of cryogenic temperatures. The production of oxygen from the fractional distillation of liquid air around 1900 was the first significant application of cryogenics. The oxygen was needed for oxy-acetylene welding, and the fractional distillation process was much cheaper than the chemical process used prior to that time [Scurlock, 1992]. The seven general benefit areas of nearly all cryogenic applications were described in the Introduction Section, and applications employing these benefits are described in the next section. Other applications were covered in the other chapters of this book.

15.3 Applications of Cryogenics

15.3.1 Long-term preservation of biological material and food

15.3.1.1 Preservation of biological material

After geneticists had refined the process of artificial insemination in cattle and other farm animals in the 1940s a major breakthrough came in England in 1949 regarding successful freezing of chicken sperm by including glycerol. Other cryoprotectors had been tried earlier without much success [Foote 2001]. Storage of frozen cattle sperm treated with glycerol was initially carried out with dry ice at 194 K, but in the 1950s liquid nitrogen became the preferred refrigerant because some biological changes were noted at 194 K but not at 77 K using liquid nitrogen.

The first successful human pregnancy using frozen sperm occurred in 1953 [Bunge & Sherman 1953] and by 1972 the first commercial cryobanks were founded. In 1983 the first pregnancy resulting from the use of a frozen embryo took place in Australia [Trounson & Mohr 1983], and twins, a boy and a girl, were born in Australia as a result of the use of frozen eggs in 1986 [Chen 1986]. A successful birth using sperm frozen with liquid nitrogen for 20 years was carried out at the Tyler Medical Clinic in 1998 [www.tylermedicalclinic.com 2005]. It is possible to store blood for over 20 years utilizing liquid nitrogen and cryopreservation agents, although the process is expensive. It is particularly useful for the storage of cord blood and stem cells. Further research is continuing in this field.

15.3.1.2 Food freezing

The freezing of food for preservation has been practiced for centuries and does not require cryogenic temperatures. However, the use of liquid nitrogen allows for quick freezing of foods, which can prevent surface dehydration and improves taste and color. Fast freezing prevents large ice crystals from forming that do more damage to cell walls than do small crystals. It also reduces the tendency for individual pieces to stick together. Cryogenic quick freezing is 3 to 4 times faster than that obtained with conventional refrigeration systems and allows for higher throughput and lower costs. Typically the fast freezing is carried out with the food placed on a flat belt that moves into a tunnel with cold nitrogen vapor passing over the food before further cooling with the spray of liquid nitrogen. Flat belt LN_2 tunnels are designed so that the LN_2 is sprayed on the food product at the exit end of the freezer, and the cold vapor forced back towards the entrance of the freezer. In this way, the available refrigeration in the vapor is used most efficiently. **Figure 1** shows an example of such a tunnel freezer. Typical liquid nitrogen flow rates in one of these systems vary from about 200 to 2000 kg/hr. The fast freezing techniques and equipment became especially popular when liquid nitrogen supplies were readily available beginning in the 1960s.

Figure 1: Liquid nitrogen fast food freezer. Courtesy Air Liquide.

15.3.2 High Density Fluids (liquefaction and separation)

15.3.2.1 Air separation

The benefit of liquefaction to separate oxygen and nitrogen from air by distillation was the first application of cryogenics, which appeared around 1900 to provide large quantities of low cost oxygen for the welding industry. The air separation industry had grown to a rather large size by 1950, and it has continued to grow rapidly in the last 50 years. The liquefaction of a gas increases its density by about 600 to 900 times compared to the gas at ambient temperature and pressure. Thus, much smaller volumes are needed for the same energy or mass of fluid. The shipping of large quantities of gas is much more economical if done in liquid form.

Figure 2 shows how oxygen production in the USA has grown by about a factor of 30 compared with that in 1954 [Royal 2005]. Nitrogen has grown even faster, increasing from 0.53 x 10^6 tonnes in 1960 to 21.3 x 10^6 tonnes in 1985, a factor of 40 [Baker & Fisher 1992, Bureau 2005, Grenier & Petit 1986]. Data after 2005 is now difficult to obtain because the US Census Bureau discontinued its report on industrial gases in 2005. The typical size of an air separation plant increased from about 100t/d in 1954 to about 500 t/d in 2005, but the largest is now about 4000 t/d from a single train. A large eight-train facility in Qatar produces 30,000 t/d of oxygen. Cryogenic Air Separation Units (ASU) are used in medium and large-scale plants and for high purity (98 to 99.5 %) gases. A cryogenic ASU is more economical than Pressure Swing Absorption (PSA) or membrane processes for systems larger than about 60 t/d and for high purities. **Figure 3** shows a modern cryogenic air separation plant that also includes a liquid hydrogen system. Liquid hydrogen production uses liquid nitrogen precooling, so the two facilities are often located together. Large deliveries of any of these gases are only economical if carried out in the liquid form, as shown by the insulated tank truck in this figure. **Figure 4** compares the oxygen demand in Japan from various industries [Kato et al 2003]. This figure shows that the steel making industry with their blast furnaces (basic oxygen furnace) and electric furnace dominates the oxygen market. **Figure 5** shows the production rate of oxygen, nitrogen, and crude steel in Japan between 1960 and 1985 [Oshima & Aiyama 1992]. We see the oxygen demand follow closely to the production of crude steel. **Figure 6** shows the world production of crude steel from 1950 to 2013 [World Steel 2014]. The rapid increase since about 1995 is driven by much new construction in China, which now is the world's largest producer and consumer of steel [World Steel 2014].

Liquid oxygen is used in the space program as an oxidizer in rockets but the total amount used is less than about 5 % of the total USA oxygen production. In 1965 the USA space program consumed 0.40 x 10^6 tonnes of liquid oxygen compared with the total USA production of 6.8 x 10^6 tonnes. For this application it is the much higher density of the liquid phase that enables the use of pure oxygen in rockets. For exploration of the solar system with return capabilities, such as manned missions to Mars, the production of liquid oxygen on Mars will be an important part of the mission. The oxygen would be generated chemically from the carbon dioxide atmosphere, liquefied, and then stored in empty tanks brought on board the lander. Very efficient and reliable oxygen liquefiers will be required for such a mission [Marquardt & Radebaugh 2000]. Recent developments in space cryocoolers in the last ten years can satisfy these difficult requirements.

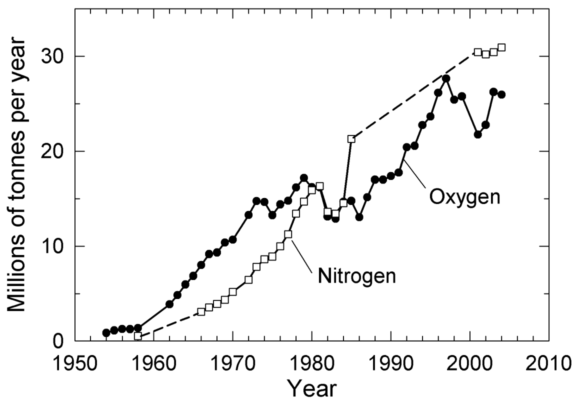

Figure 2: Annual US oxygen and nitrogen production.

Figure 3: Modern air separation plant with hydrogen liquefaction. Photo courtesy Praxair.

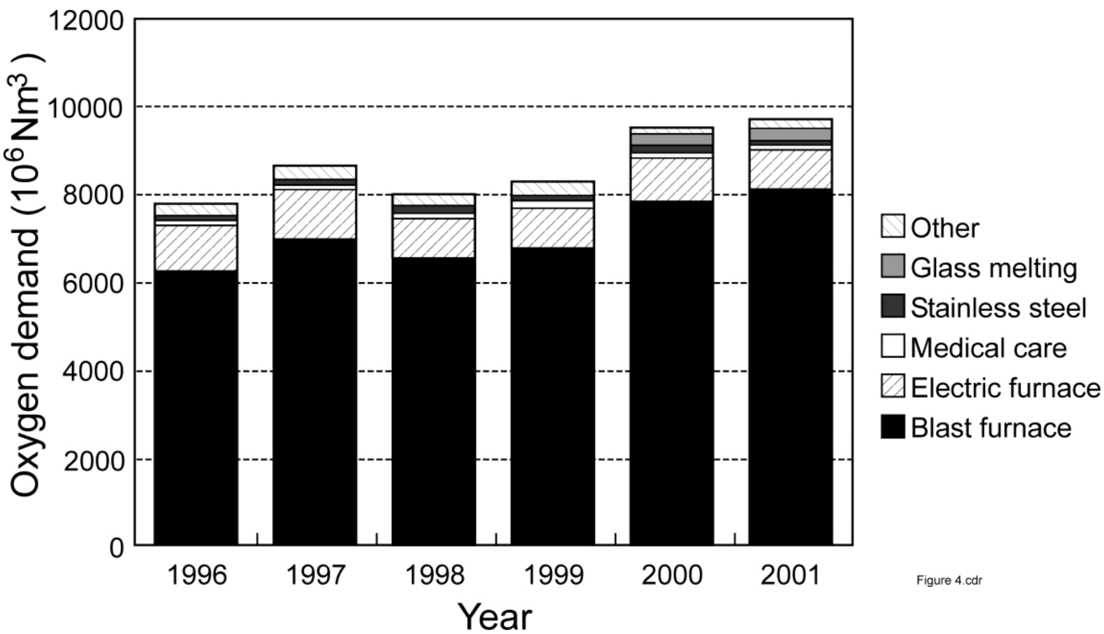

Figure 4: Japanese annual oxygen demand and usage. Data from Kato et al. 2003.

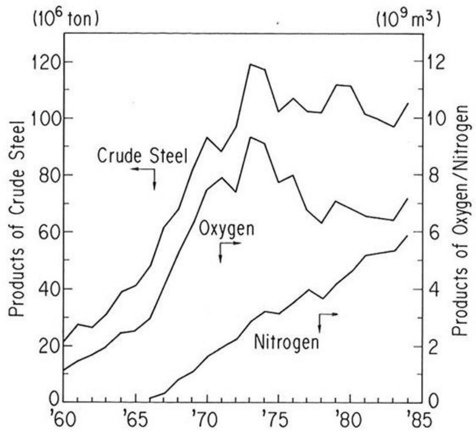

Figure 5: Oxygen, nitrogen, and steel production in Japan.

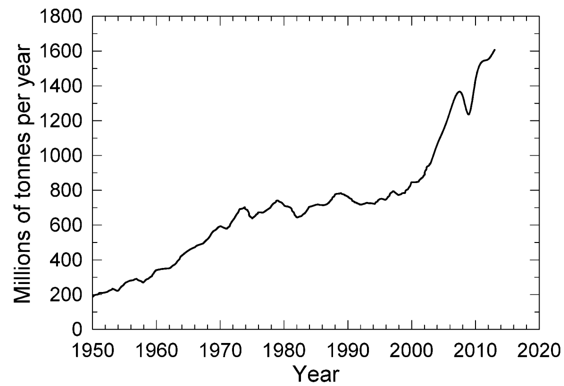

Figure 6: Annual world crude steel production.

The large increases in the use of nitrogen in the last 20 to 30 years has been driven by the food freezing industry (discussed earlier), as an inerting gas in the stainless steel and semiconductor industry, and to pressurize oil wells to increase the extraction rate. In fact one of the world's largest air separation plants (3000 t/d) is for the purpose of nitrogen gas pressurization of oil wells off the coast of Mexico. Air separation plants in the US required about 50 x 10^{15} J of electrical energy in 2004 [ORNL 2005] about 0.35 % of the total US electrical energy output at that time. The total value of oxygen, nitrogen, argon, and hydrogen produced in the US in 2002 was about $4 billion [Bureau 2004].

15.3.2.2 Liquid Hydrogen

Demands for liquid hydrogen began to increase rapidly after about 1958 to provide the rocket fuel needed for the space programs of many countries. The first space flight of Sputnik I by the Soviet Union in 1957 initiated the space age with many countries developing capability to send satellites into space over the next several years. The 'Papa Bear' hydrogen liquefier established in Florida for the secret Air Force program on a hydrogen fueled airplane was ready to supply liquid hydrogen for NASA's development of rocket engines after cancellation of the Air Force program [Sloop 1978]. Additional hydrogen liquefiers were built soon after 1960 and by 1965 the USA hydrogen liquefaction capacity reached 200 t/d compared with 14 t/d in 1959 [Tishler 1966].

For the manned mission to the moon NASA developed the Saturn V rocket with three stages. The first stage engine was fueled with kerosene and liquid oxygen and produced a thrust of 33.4 MN. The second and third stages were fueled with liquid hydrogen and liquid oxygen with thrusts of 5 MN and 1 MN, respectively. In July, 1969 the Saturn V carried Apollo 11 to the moon for the first manned lunar landing. The launch is shown in **Figure 7**. About 50 % of the liquid hydrogen used by NASA for flight operations is lost because of transient chilldown of warm cryogenic equipment, purging, and heat leaks into ground storage tanks, transportation vessels, flight vessels, and transfer lines. A new project under development at NASA/ Kennedy, called Integrated Ground Operations Demonstration Unit for Liquid Hydrogen (GODU-LH2) aims to decrease the loss to less than 20 %. It includes onsite refrigeration to provide zero boiloff of storage tanks and densification of the liquid by chilling to 16 K [Notardonato 2014].

A 1990 NASA study indicated the USA liquid hydrogen production rate was 140 t/d that year. By 2008 the rate had increased to about 210 t/d [EPA 2008]. The largest hydrogen liquefiers today can produce about 20,000 L/hr or about 34 t/d. The total US production rate of hydrogen was about 3000 t/d in 2001 and 4100 t/d 2004, but most of the hydrogen is used onsite for oil refining or ammonia production [Bureau 2005]. If the hydrogen economy were to progress, the production rate of hydrogen will increase dramatically, and so will the liquefaction rate. At this time studies show that because of its high density, liquid hydrogen fueled automobiles provide the greatest range compared with other hydrogen storage methods, such as compressed gas or metal hydrides. New automotive hydrogen dewars with liquid air shielding show zero boiloff hold times of up to two weeks [Trill 2002].

Figure 7: Launch of Apollo 11 to moon with Saturn V rocket (NASA photo)

15.3.2.3 Liquefied Natural Gas

Liquefied natural gas (LNG) was first exported from Lake Charles to Canvey Island, United Kingdom in 1959 via a converted crude-oil tanker re-named the *Methane Pioneer* with free-standing aluminum tanks and insulated with balsa wood and fiber glass [Haselden 1992]. The total load was 5000 m^3.

In 2002 the U.S. produced 84 % of its total natural gas needs, with most of the remainder coming via pipeline from Canada. In that year about 1 % of the total U.S. supply was imported as liquefied natural gas (LNG) from overseas via ship. After about 2005 the production of natural gas in the US increased dramatically because of the hydraulic fracturing of shale gas fields and the use of horizontal drilling. **Figure 8** shows this rapid increase in US natural gas production. Previous to that time the Energy Information Administration (EIA) of the Department of Energy (DoE) had predicted that by 2025 LNG imports would contribute about 21 % of the US natural gas needs. As of 2012 EIA now predicts an export of LNG from the US amounting to about 10 % of the US production in 2015, as shown in **Figure 8** [DOE/EIA 2014].

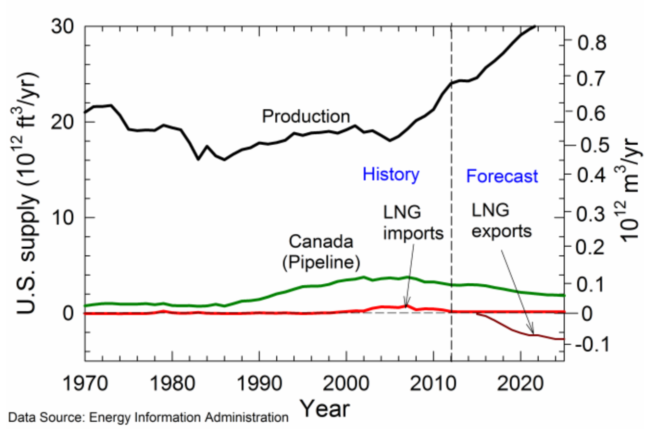

Figure 8: U.S. annual natural gas supply. Data from EIA/DoE

As of 2005 there were only four LNG marine receiving terminals in the U.S.: (1) Everett, Massachusetts, built in 1971, (2) Cove Point, Maryland, built in 1978, (3) Elba Island, Georgia, built in 1978, and (4) Lake Charles, Louisiana, built in 1982. **Figure 9** shows the Elba Island facility in 2004 before completion of the new unloading docks to the left in a channel off from the main Savannah River. The total storage capacity of all four of these facilities is currently 0.53 billion m^3 (18.8 billion ft^3) (gas equivalent), sufficient for only 8 hours of the U.S total natural gas usage. In 2014 there were 11 import terminals in the U.S., but because of the rapid increase in domestic natural gas production that started around 2005, many of these facilities are adding liquefaction plants and export capability [CLNG 2015]. The oldest active marine terminal in the U.S. was constructed in Kenai, Alaska, in 1969 to export LNG to Japan, the creators of the world LNG market. The Kenai facility has a liquefaction plant, whereas the 11 receiving terminals currently have only vaporizers. In 2005 there were 57 storage facilities in the U.S. with liquefaction plants for use in peak shaving and another 56 smaller niche-market LNG facilities. Because of the rapid increase in US natural gas production, the demand for the import LNG facilities rapidly decreased except for certain regions, such as the northeast U.S. However, there are now nine sponsors of applications for LNG export facilities in the US. One is now under construction next to an import facility at the Sabina Pass terminal in Louisiana and is expected to be online by the end of 2015. When finished it will have four liquefaction trains for a total liquefaction capacity of 77.8 million m^3/d (2.76 Bcf/d). Two more liquefaction trains are scheduled to be added later. Each train has a liquefaction capacity of about 4.5 million tonnes per annum (mtpa).

Figure 9: Elba Island (Savannah) LNG import terminal and regasification facility. Photo courtesy Southern LNG.

On May 21, 2003, Alan Greenspan, Federal Reserve Chairman said, "Our limited capacity to import liquefied natural gas effectively restricts our access to the world's abundant supplies of natural gas." Preparations to bring about an enormous increase in LNG supply to the U.S. began in the early to mid-2000s. As of July 2005, there were more than 50 proposals for new receiving terminals in the U.S., but those proposals were quickly abandoned as the US production rapidly increased. Currently, Japan has 23 receiving stations and obtains nearly 100 % of its natural gas as LNG. Many other countries with insufficient natural gas reserves are now looking to follow in Japan's footsteps by importing LNG to at least supplement their domestic production. The LNG market then begins to mimic the oil market and will play a significant role in global energy supplies in the 21st century.

To meet the growing demands for global natural gas requires a large increase in the number of LNG ships and liquefaction facilities. At the end of 2011 there were 359 LNG tankers in operation worldwide, most of them with capacities of 120,000 m^3 (liquid) or more. There are 55 new ships under construction with 46 of them having a capacity of 138,000 m^3. These ships are among the most complex and expensive merchant ships ever built, but the construction costs have decreased from about $270M in 1990 to about $155M in 2005. The length of a typical LNG tanker is about 300 m (1000 ft). **Figure 10** shows one type of LNG tanker (Al Wajbah) built in 1997 with five spherical storage tanks for a total capacity of 137,000 m^3 for shipments from Qatar to Japan. The other major type contains the liquid within the hull and uses a membrane. About 0.15 to 0.25 % of the LNG being transported boils off each day and is used to partially fuel the ship. Typically about 1 to 5 % of the cargo boils off during a shipment (depending on the distance traveled). The shipping cost is about 10 to 30% of the LNG cargo value (depending on the distance traveled). An excellent review of the LNG shipping industry and market is given in a report by Alavi with DVB [DVB 2003].

A new approach to the processing, liquefaction, and exporting natural gas is the development of Floating Liquefied Natural Gas (FLNG) platforms. Construction on the first one (known as Prelude) began in 2012 and is expected to be operational 200 km off the northwest coast of Western Australia in 2017 [Schilling 2014]. Construction cost is expected to be $52 billion. It is 488 m long, which makes it the largest ship in the world. It will extract, process, liquefy, and offload LNG and other liquid products as it is moored above the Prelude and Concerto gas fields in the Browse Basin. It will produce 3.6 million tonnes per annum (mtpa) of LNG, 1.3 mtpa of condensate, and 0.4 mtpa of LPG. Plans for several other FLNG platforms are under study.

Figure 10: LNG tanker Al Wajbah (137,000 cubic meters) traveling between Qatar and Japan.

15.3.3 Macroscopic quantum phenomena (superconductivity and superfluidity)

Decreasing the temperature of any material has the effect of reducing the thermal excitations of the atoms. At sufficiently low temperatures, the thermal excitations can become less than some quantized first energy level. The atoms or pairs of atoms may then 'condense' into the lowest energy in which their de Broglie wavelengths become very long and overlap with other atoms. The interaction causes a coherence of the atoms such that they can move together as one and take on entirely different properties than at higher temperatures. Such quantum effects in bulk systems are unique to low temperatures. The two common examples are superconductivity where there is no resistance to the flow of electricity and superfluidity where there is no resistance to the flow of the fluid and the thermal conductivity is extremely high. Superconductivity, in particular, has many very useful applications.

15.3.3.1 Bulk superconductor applications

Soon after the discovery of superconductivity by Onnes in 1911 at a temperature of 4.2 K in mercury, other metals were found that were also superconducting. Unfortunately, the superconducting state would revert back to the normal state with rather low values of applied magnetic fields. The critical fields of the pure elements are less than about 0.2 T at 0 K so they are of little use in carrying large currents and generating high magnetic fields. Metallic alloys and compounds were also studied between 1911 and 1950 and found to have higher critical temperatures and fields. In 1953 V_3Si was discovered to have a critical temperature of 17.5 K, the highest value at that time. The critical magnetic field in V_3Si near 0 K is about 2.3 T, too low for useful magnets. The materials were also difficult to make into wire form. In addition, only few laboratories at that time had the ability to achieve temperatures of 4.2 K that would be required for any superconducting magnet. Thus, in the 1950s there were no practical applications of superconductivity. In fact, there were no theories available at that time to satisfactorily explain superconductivity.

Figure 11 gives a time line of the important discoveries and applications dealing with bulk superconductivity after 1950. The first was the discovery by Matthias in 1954 of Nb_3Sn with a transition temperature of 18 K, the highest at that time [Matthias et al 1954]. The BCS theory [Bardeen et al 1957] of superconductivity was then published in 1957, 46 years after superconductivity was discovered by Onnes. A very significant discovery was made in 1961 that quickly led to applications of superconductivity. The superconducting compound Nb_3Sn that was found 7 years earlier to have such a high transition temperature was found to have a critical field in excess of 8 T at 4.2 K, about an order of magnitude higher than anything found before [Kunzler et al 1961]. Unfortunately, it was very brittle and difficult to fabricate. A year later the ductile alloy NbTi was found by scientists at Westinghouse to be superconducting at 9.5 K and to have an upper critical field of about 11 T at 4.2 K [Hulm & Blaugher 1961]. Most importantly it was a ductile alloy easily fabricated into wires. It became the first commercial superconducting wire.

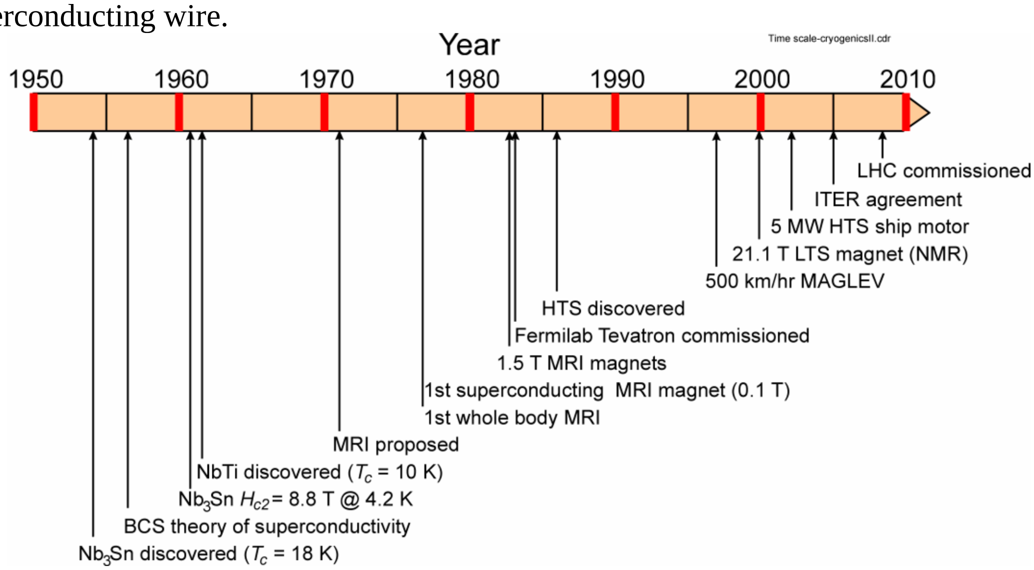

Figure 11: Time line for significant discoveries or inventions dealing with bulk superconductivity.

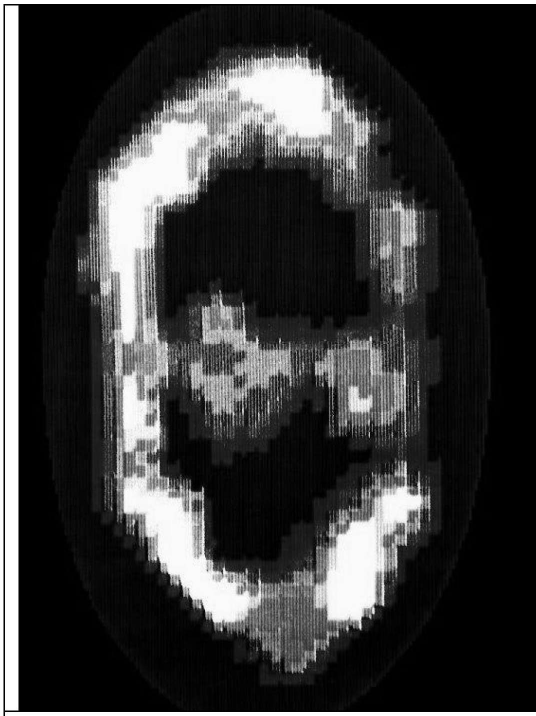

Figure 12: First whole body MRI image, taken of the lung cavity in 1977.

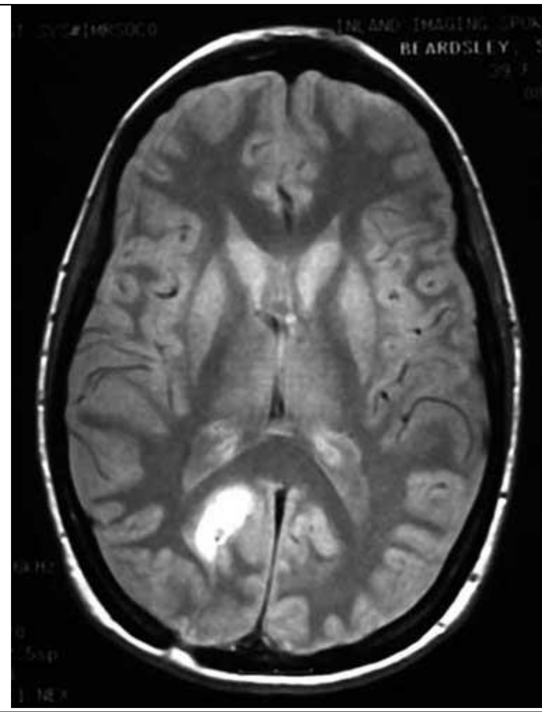

Figure 13: Recent MRI image of the brain showing a brain tumor in white.

By the mid-1960s liquid helium had become readily available either through use of the commercial Collins helium liquefier or through air shipments of liquid helium from large liquid helium suppliers, which afforded the first significant commercial application of superconducting magnets for magnetic resonance imaging (MRI) [Schwall 1987]. In 1971 Raymond Damadian showed that the nuclear magnetic relaxation times of tissues and tumors differed [Damadian 1971] thus motivating scientists to consider magnetic resonance for the detection of disease. Magnetic resonance imaging was first demonstrated on small test tube samples in 1973 by Paul Lauterbur [Lauterbur 1973]. A whole body image [Damadian 1977] of the chest, shown in **Figure 12**, was first made in 1977 using the system patented by Damadian [Damadian 1974] in 1974, which utilized a NbTi superconducting magnet consisting of a 1.3 m diameter Helmholtz pair that reach a maximum field of 0.10 T [Goldsmith et al 1977]. Improved imaging techniques were introduced by others [Kumar et al 1975; Mansfield 1977; Mansfield & Maudsley 1976] that are in common use today. A recent MRI image showing a brain tumor is given in **Figure 13**. Some of the early MRI systems used normal or permanent magnets, which could provide fields of 0.15 T, but greatly improved resolution was provided by going to 1.5 T, which could only be provided by NbTi superconducting magnets. Most systems today use 1.5 T superconducting magnets, but there are a few new systems with 3.0 T magnets. MRI has now become the largest commercial application of superconductivity with over 22,000 superconducting MRI systems in operation worldwide. Approximately 1000 systems per year are sold [Muller and Hopfel 1998] at a cost of about $2 million each. About 100 t/yr of NbTi are required to produce the superconducting magnets [Scanlan et al 2004]. Considering the magnetic fields required for good images, normal magnets simply cannot compete. **Figure 14** shows a typical MRI system of today which uses a field of 1.5 T. Two-stage Gifford McMahon cryocoolers capable of providing 1.5 W at 4.2 K are often used to eliminate any liquid helium boiloff. About 7000 such cryocoolers had been sold between 1995 and 2003 [Kuriyama 2003]. **Figure 15** shows the rapid growth of MRI systems from 1980 to 2004 and again since about 2012 [Andrews 1988; Devred et al 1998; Schwall 1987; Week 2005; Magnetic Resonance 2015; CCAS 2015) The field is expected to see continued steady growth, especially as newer applications develop in the identification of Alzheimer's disease and multiple sclerosis. The MRI and NMR markets dominate the worldwide superconductivity market, which is projected to exceed about US$8.8 billion by 2020 [Global Industry Analyst 2015].

Nuclear Magnetic Resonance (NMR) is used in MRI for imaging. It can also be used for spectroscopy to analyze biomacromolecules. Over the past fifty years NMR has become the preeminent technique for determining the structure of organic compounds, especially proteins. There are two main ways to study the structure of proteins – NMR spectroscopy and x-rays crystallography. X-ray crystallography can be used only with proteins that can be made into single crystals, which include about 75% of the 50,000 to 100,000 proteins existing in the human body. The structure of the remaining proteins can be determined only by the use of NMR spectroscopy. This technique can be used for proteins in solution, that is, in an environment similar to that in a living cell. In fact the use of this technique for the study of protein structure and function led to two Nobel Prizes in Chemistry, one to Richard Ernst in 1991 and one to Kurt Wuthrich in 2002. Very high magnetic fields are required for NMR spectroscopy of large macromolecules like proteins. A magnetic field of 21 T is required for resonant frequencies of 900 MHz, which allows study of proteins with molecular weights up to about 30,000. **Figure 16** shows an example of a 900 MHz NMR system. In order to study heavier proteins higher resonance frequencies are required, which in turn requires higher magnetic fields. A system operating at 1 GHz frequency with a magnetic field of 23.5 T has been introduced in the last couple of years. Obviously, such high magnetic fields are only possible with superconducting magnets. The magnets are made with a Nb_3Sn coil inside a NbTi coil and the helium bath is vacuum pumped to a temperature of about 2.2 K. Many laboratories throughout the world are now using high-field NMR spectrometers for protein studies. One magnet supplier states that over 6000 of their superconducting magnets are being used for such studies. It would appear that many more such magnets will be needed for this rapidly growing field of research, especially for magnets with fields of 21 T or higher.

Figure 14: Modern MRI system with a 1.5 T superconducting magnet and cryocooler.

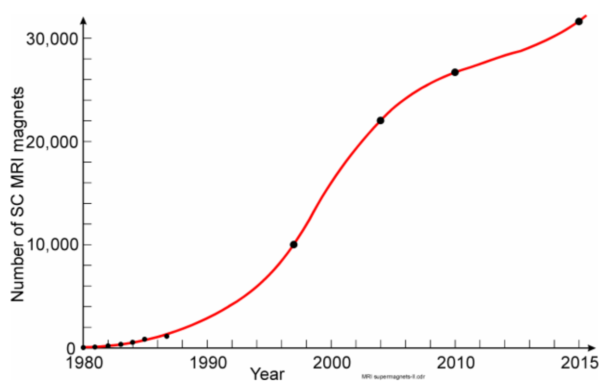

Figure.15: Cumulative number of MRI systems in use around the world.

Figure 16: 900 MHz (21.1 T) NMR system. Photo courtesy Varian.

At about the same time MRI systems with superconducting magnets were being developed, the Fermilab Energy Doubler or Tevatron was under construction using about 1000 NbTi superconducting magnets in a ring of 6.3 km circumference to bend and focus the proton beam [Edwards 1985]. The dipole magnets for bending the beam are 6.1 m long and provide a magnetic field of 4.4 T [Gourlay et al 2004]. To cool the magnets the helium liquefier system (central plant plus satellites) delivers a peak refrigeration power of 24 kW at 4.5 K through a circuit of 27 km. The Tevatron was commissioned in 1983 and named in 1993 as an International Historic Mechanical Engineering Landmark by the American Society of Mechanical Engineers. Since then many other high energy physics accelerators have used superconducting magnets. The largest, completed in 2008 in Switzerland at CERN, is the Large Hardon Collider (LHC). It is the most powerful accelerator ever built, in which two counter rotating beams of protons at energies of 7 TeV each can be made to collide head on. Its ring circumference is 27 km and each of the 1232 NbTi dipole magnets are 14.2 m long [Gourlay et al 2004]. According to CERN, an energy of 1 TeV is equivalent to the energy of motion of a flying mosquito, but with the LHC the 14 TeV is concentrated into a volume about 10^{12} times smaller than a mosquito. The high energy concentration splits the proton into elementary particles that help us understand the structure of the early Universe. A particle matching the Higgs boson was already discovered in 2013 with the LHC running at about half its rated power. It is expected that several new particles will be discovered with the LHC when it is run at full power starting in 2015. **Figure 17** shows the assembly of one LHC dipole section surrounded by its vacuum can. Each of the 392 quadrupole magnets are 3 m long. About 7000 km of superconducting wire was required for all the magnets. If normal magnets had been used the ring circumference would have been 120 km, and the required input power would have been astronomical. The specified magnetic field is 8.36 T, which requires the magnets be cooled to about 1.9 K in superfluid helium in order to achieve the higher field. The total mass to be cooled is 37,000 tonnes. The quantum nature of superfluid gives it enormous thermal conductivity (hundreds of times that of OFHC copper), extremely low viscosity, and a specific heat about 10^5 times that of the superconducting magnets per unit mass. The helium liquefier plant is split into eight liquefier stations spaced around the ring, each of which services about 3.3 km of the ring. **Figure 18** shows a portion of the ring where the helium lines connect into the main ring from an auxiliary helium line. Both 4.5 K liquid and 1.9 K liquid at 0.13 MPa (1.3 bar) are produced at each station. The heat load on the 1.9 K superfluid helium is about 2.3 kW for each station. The total equivalent 4.5 K refrigeration capacity for the complete ring is 144 kW, which makes the LHC the world's most powerful helium refrigeration system. The total input power is about 40 MW [Delikaris and Tavian 2014].

Figure 17: One dipole magnet being assembled into a cryostat for the LHC at CERN. The two tubes near the center are the two beam tubes. Image: CERN.

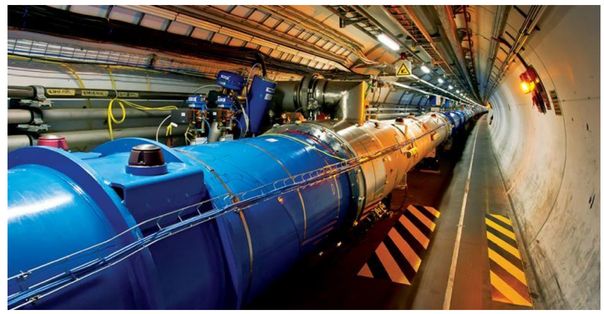

Figure 18: The LHC tunnel and dipole magnet sections at CERN. Superfluid helium is supplied to the tubes from the tower located behind the beam path. Image: CERN

Superconducting magnets are often used in particle detectors also because observing a particle's trajectory in a magnetic field is the easiest way to determine its momentum. The magnetic field is the easiest tool to determine the momentum of a particle by observing its trajectory in the field. In the LHC the high energy protons collide in four regions around the ring, housing four unique detector experiments. The two largest experiments, ATLAS and CMS, will use superconducting magnets. The ATLAS detector is the largest ever built for particle physics. The barrel toroid has an outer diameter of 20.1 m and a length of 25.3 m [Gourlay et al 2004]. The peak field is about 3.9 T. The CMS detector uses the largest solenoid ever built. It has a central field of 4 T with a diameter of 6 m and a length of 12.5 m.

Superconducting magnets are also used in magnetic confinement systems for fusion studies and in some inertial confinement systems. International agreement was obtained in 2005 for the location of the International Thermonuclear Experimental Reactor (ITER), the largest of the tokamaks under design by an international collaboration. A tokamak is a device that uses a magnetic field to confine a plasma in the shape of a torus. It has a plasma major radius of 6.2 m and a minor radius of 2 m. The toroidal field at the major radius is 5.3 T, but fields of 12 to 13 T are required at other locations [Gourlay et al 2004]. The higher fields are generated with Nb_3Sn magnets, whereas the lower fields are generated with NbTi magnets [Shimomura 2001]. All coils are cooled with supercritical helium that is forced through the tubes containing the cables at a temperature of 4.4 to 4.7 K. The liquid helium is produced by four identical liquid helium modules similar to the modified CERN 18 kW helium refrigerators [Kalinine et al 2004].

One of the most interesting applications of superconductivity is for magnetic levitation. Levitation can be accomplished with either an attractive system, called Electro Magnetic Suspension (EMS), which requires feedback control or with a repulsive system, called Electro Dynamic Suspension (EDS), which is inherently stable and requires no feedback control. The attractive systems can use normal magnets, such as those used in the Maglev monorail train between Shanghai and the Shanghai Pudong International Airport, a distance of 30 km. The regular speed is 430 km/hr, although it has achieved a top speed of 501 km/hr. It is the fastest commercial railway system in the world. The repulsive (EDS) system has the advantage of simpler control systems and a levitated height of about 10 cm, thus relaxing the requirement on the straightness of the guide way. Japan began experimental work on a superconducting EDS system in 1972 that achieved the 10 cm levitation with a maximum speed of 60 km/hr. The current test trains travel nominally at 500 km/hr on the 43 km long Yamanashi Test Track, although a top speed of 581 km/hr was achieved in 2003 with a manned three-car test train. Non-paying passengers have been invited to ride the five car test train since 2001, and in 2004 the cumulative traveled distance exceeded 400,000 km. **Figure 19** shows the 2003 five-passenger test train, which the author was invited to ride in 2003 at a speed of 500 km/hr. There are 4 NbTi magnets in each cryostat, and one cryostat is placed on each side of the coupling between two cars. Each cryostat requires 7 W of refrigeration at 4.2 K, which is provided by a helium JT cryocooler precooled with a Gifford McMahon cryocooler. The 'track' is a U-shaped guideway with two sets of aluminum rings on each wall. As the superconducting magnet passes by one set at a speed greater than about 50 km/hr it levitates the train. An electromagnetic wave travels along the other set of rings in the guideway to propel the train like a surfboard riding a wave [Railway 2004]. In late 2005 one of the LTS magnets was replaced with a Bi2223 HTS magnet with the same field of 1 T, but operating at 20 K by direct conduction cooling with a Gifford-McMahon cryocooler. Performance of the train was not changed Kuriyama 2005]. In 2011 the Japanese government granted JR Central permission to operate their SCMaglev system between Tokyo and Nagoya by 2027 and to Osaka by 2045.

Figure 19: Japanese Maglev train that uses superconducting magnets for levitation and has a rated speed of 500 km/hr. Image: Central Japan Railway Company

In 1986 a breakthrough discovery was made in the field of superconductivity. Bednorz and Muller found that a brittle ceramic compound became superconducting at temperatures around 30 K [Bednorz & Muller 1986]. A flurry of activity ensued and similar materials with much higher critical temperatures T_c were found. One year later the material $YBa_2Cu_3O_7$, known as YBCO, was found to be superconducting at 92 K, the first superconductor to have a transition temperature above liquid nitrogen temperature [Wu et al 1987] subsequent measurements on this material showed it to have an upper critical field at 0 K of about 130 T. This material is now being manufactured as tape and is called second generation HTS wire. It can be operated at temperatures of about 50 to 70 K, depending on the magnetic field strength. In 1988 the ceramic $Bi_2Sr_2Ca_2Cu_3O_{10+\delta}$, known as BSCCO-2223, was discovered to have a transition temperature of 110 K [Maeda et al 1988]. This superconductor is marketed as first generation HTS tape for power and magnet applications. It has a lower critical field than YBCO and must be operated at about 30 to 35 K for high field applications. **Figure 20** compares the upper critical field of useful LTS and HTS materials [Scanlan et al 2004]. The highest confirmed T_c is 138 K discovered in 1995 in a thallium-doped mercuric cuprate [Dai et al 1995].

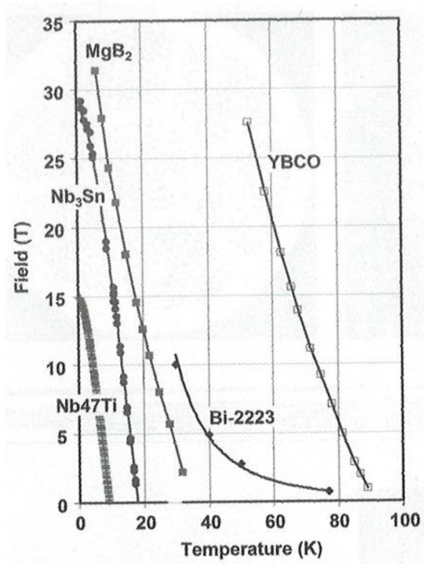

Figure 20: Upper critical magnetic field for several practical superconductors. From Scanlan et al. 2004

The high temperature superconductors are now being developed into many large scale power applications, such as motors, generators, transformers, synchronous condensers, fault current limiters, and transmission lines [Malozemoff et al 2005]. Several demonstration AC transmission lines have been tested or are being developed in many countries. In early 2005 a 500-m 77-kV single phase HTS cable was tested in Japan. In the US a consortium of companies built a 660-m, 138-kV HTS cable to connect to the Long Island Power Authority grid. It became operational in 2008. The primary advantage of HTS cables is their much higher rms current density of 10,000 A/cm^2 compared with 100 A/cm^2 for copper cables. After adding the dielectric, cryostat, and structure, the HTS cables can still carry about 2 to 5 times that of conventional cables [Malozemoff et al 2005]. As a result in urban areas where underground utilities are crowded, additional electric power can be added simply by replacing the conventional cable in a given conduit with a HTS cable. Currently, expensive 1st generation BSCCO cables are being used, but soon sufficient lengths of lower cost 2nd generation YBCO cables will be available. Typically cooling is accomplished with forced flow of liquid nitrogen subcooled to about 65 K to eliminate two phase flow. The refrigeration power is typically about 10 kW at 65 K for these test transmission lines.

The use of HTS in rotating machinery, such as generators or motors offers the advantage of reduced losses, weight, size, and cost. The need for a cryocooler with HTS systems restricts the usefulness of such systems to those larger than about 1 MW. In the case of large motors or generators the losses may be reduced by a factor of two compared with conventional motors or generators, but even conventional machines are quite efficient. The major advantage is HTS machinery can be about 1/3 the weight and volume of conventional machines of the same power [Malozemoff et al 2005]. Such size reductions are particularly attractive for use in ships. A demonstration model 5 MW HTS ship motor with a speed of 230 rpm was constructed and tested in 2003 using BSCCO wire and operating at about 35 K. The higher magnetic field in motors and generators compared with transmission lines means that they must operate at a lower temperature compared with transmission lines (see **Figure 20**). The largest superconducting motor developed to date is a 36.5-MW, 120-rpm ship propulsion motor (about 50,000 hp). Such a motor is sufficiently large to use on passenger cruise ships as well as larger military vessels. **Figure 21** compares the size of such a motor to that of a conventional motor of the same power. The much smaller size of HTS motors makes way for greater cargo or passenger capacity. **Figure 22** shows the rapid increase in size of developmental HTS motors since 1990. Industry analysts estimate that the electric drive market for ship propulsion to grow to about $2.4 billion annually in the next 10 years. HTS motors are expected to capture about one-half of that market [Corporation 2005]. A thorough review of both LTS and HTS motors and generators is given by Kalsi *et al.* [Kalsi et al 2004].

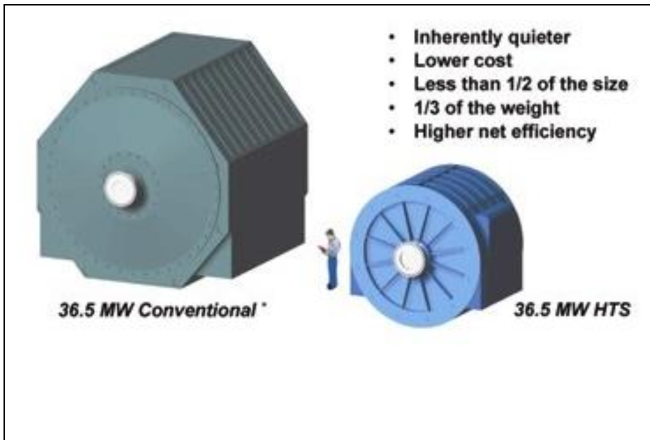

Figure 21: Size comparison between a conventional ship motor and a superconducting ship motor. Courtesy AMSC

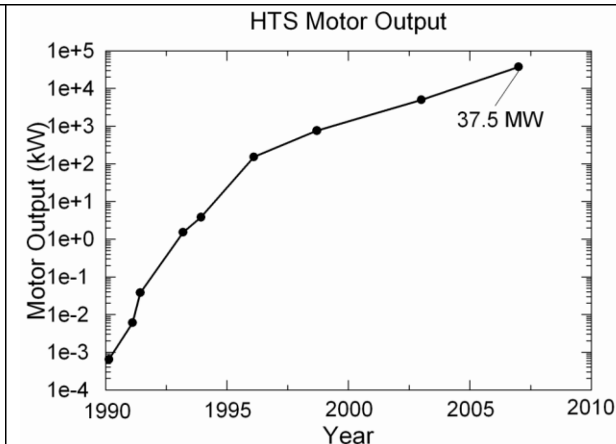

Figure 22: HTS motor output versus year.

15.3.3.2 Electronic applications of superconductivity

Figure 23 summarizes the important discoveries or inventions in the last 50 years that have had a major influence on the development of electronic applications of superconductivity. The better understanding of superconductivity that came with the BCS theory [Bardeen et al 1957] in 1957 was instrumental in leading Brian Josephson to predict in 1962 that a junction of two superconducting electrodes separated by a thin insulating barrier would allow Cooper pairs to tunnel through the barrier with a zero voltage difference as long as the current was less than some critical value [Josephson 1962]. A voltage would appear for currents greater than the critical value. The long-range order associated with the quantum nature of supercoductivity could pass through the thin insulating junction and maintain coherence between the two superconductors. The prediction was verified experimentally in 1963 [Anderson and Rowell

1963; Shapiro 1963]. This Josephson tunneling behavior is the foundation for most electronic applications of superconductivity.

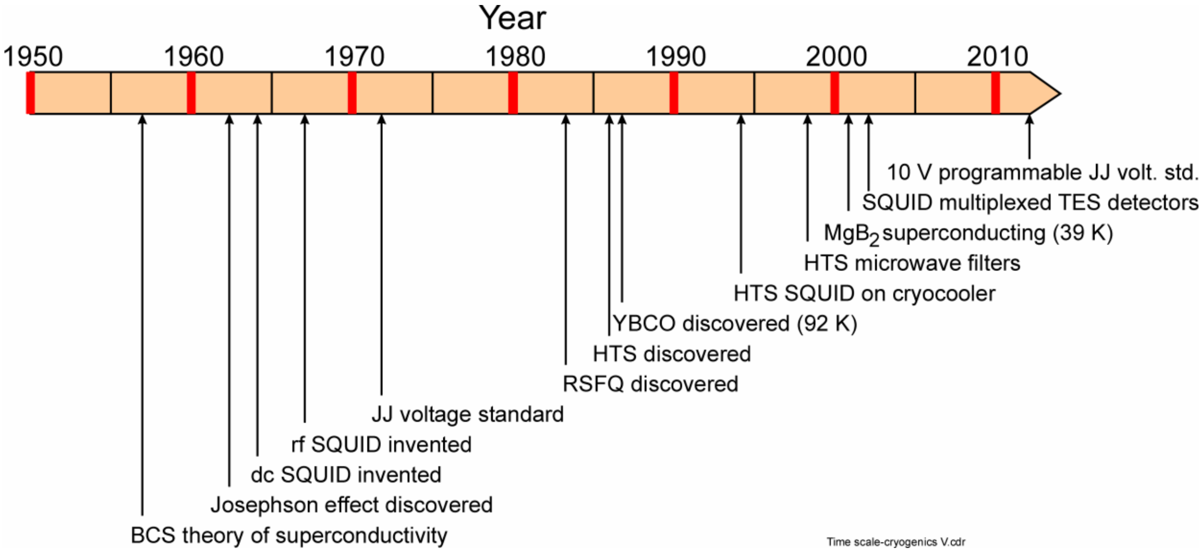

Figure 23: Time line for significant discoveries or inventions dealing with superconducting electronics.

In 1964 the superconducting quantum interference device (SQUID) was invented. The first type invented was the dc SQUID, which consists of two Josephson junctions in parallel connected by a superconducting loop and operating in the voltage state with a current bias [Jaklevic et al 1964]. An increase in the magnetic flux through the superconducting loop causes the voltage to oscillate with a period of the flux quantum $\Phi_0 = h/2e = 2.07 \times 10^{-15}$ Tm^2, where h is Planck's constant and e is the electron charge. A count of the voltage peaks determines the number of flux quanta and the resulting magnetic field. The small size of the flux quantum gives the dc SQUID extreme sensitivity to small magnetic fields. By detecting a small change in voltage within a single quanta, one typically can determine a change in magnetic flux as small as $10^{-6}\Phi_0$. The second type of SQUID is the rf SQUID, invented in 1967 [Silver & Zimmerman 1967]. It consists of a superconducting loop with a single Josephson junction. The loop is then inductively coupled to the inductor of an *LC*-resonant circuit that is driven with a rf current in the range of a few tens of megahertz to several gigahertz [Kleiner et al 2004] The amplitude of the oscillating voltage is periodic in the applied flux, with a period of Φ_0. The rf SQUID typically can be used to detect flux changes as small as $10^{-5}\Phi_0$. Increased sensitivity to magnetic fields is usually achieved by using a superconducting flux transformer with a loop area much larger than that of the SQUID. The limiting magnetic field noise achieved with LTS SQUIDs is about 1 $fT/Hz^{1/2}$ [Cantor et al 1996; Drung et al 2001]. Most SQUIDs have been made with LTS materials, primarily niobium, but the advent of HTS led to SQUIDs being made with YBCO. However, the higher temperature leads to more Johnson thermal noise and less sensitivity with the HTS SQUIDs. In addition junction quality in YBCO is inferior to that with Nb, partly due to material characteristics and partly due to the very small coherence lengths at temperatures around 77 K. The lowest magnetic noise achieved at about 1 kHz with HTS SQUIDs is about 10 $fT/Hz^{1/2}$ using a flux transformer, but noise at 1 Hz is much higher [Drung et al 1996].

The extreme sensitivity of SQUIDs to small changes in magnetic flux has led to their being useful in many applications. One of the primary applications is as magnetometers for medical applications, biosensors, geological exploration, and as high frequency amplifiers. For medical applications they can be used for magnetocardiography (MCG) to study the heart or for magnetoencephalography (MEG) to study brain activity. In these applications, the SQUIDs are paired to form gradiometers to cancel out most of the effect of the Earth's dc field or magnetic noise from medium-range to far-range sources. Typically MCG can provide better information than electrocardiograms (ECG), but because ECG is usually satisfactory, there is little market for MCG with the added cost of cooling the SQUID even to 80 K for YBCO devices. An advantage of the MCG is that there is no need to attach electrodes to the patient as is the case with ECG. If the cost and electromagnetic interference (EMI) associated with a small 80 K cryocooler can be reduced, such a market could develop.

The very low magnetic signals from the brain (about 50 fT) make it difficult for conventional magnetometers to provide a useful signal-to-noise ratio for this application. Thus, SQUID gradiometers have not had much competition for this application and have found a good market in whole head MEG systems. A typical modern helmet contains an array of about 151 × 275 SQUID sensors, including a number of reference sensors for noise cancellation, all cooled with liquid helium to 4.2 K. **Figure 24** shows a commercial MEG system in use. Various stimuli such as sound, touch, and light can be used to produce magnetic signals in the brain and help locate the corresponding portion of the brain receiving that signal. MEG is most often used to map the function of the brain in the vicinity of a tumor to aid the surgeon in finding the least invasive path. Other MEG applications include the study of Alzheimer's disease, Parkinson's disease, schizophrenia, head trauma, epilepsy, and the effects of strokes.

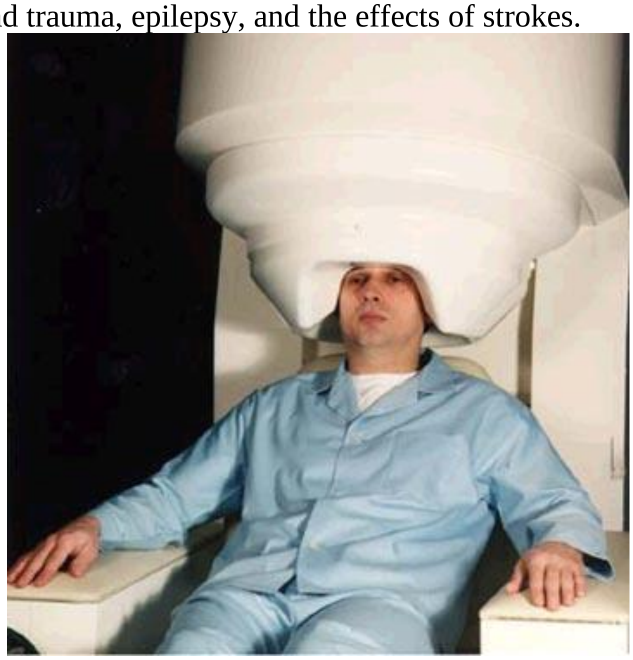

Figure 24: Superconducting magnetoencephalogram (MEG) system for brain function. Courtesy: CTF Systems.

The extreme sensitivity of SQUIDs to magnetic fields (also to voltage or current when they are coupled to a coil) makes them very useful to a wide variety of scientific measurements. In one example the presence of antigens is detected when they are selectively labeled with superparamagnetic particles. Such particles are commercially available in sizes of about 20 to 100 nm, typically consisting of a cluster of γ-Fe_2O_3 subparticles each about 10 nm in diameter [Kleiner et al 2004]. In an assay the magnetic particles are attached to the antibody appropriate to the particular antigen being sought. By applying a magnetic field and then removing it the decay rate of magnetism can be measured to determine if the particles have attached to an antigen. In one experiment a different decay rate was detected when the antigen was switched from the bacteria *Listeria monocylogenes* to *E. coli* [Grossman et al 2004]. A SQUID microscope was used for the analysis. In the microscope a sample at room temperature and pressure can be brought within about 100 to 200 µm of a high-T_c SQUID held at 77 K in a vacuum at the end of a sapphire rod that is attached to a bath of liquid nitrogen or to the tip of a mixed-gas JT cryocooler. A thin sapphire window separates the sample from the SQUID [Grossman et al 2004; Kleiner et al 2004].

Josephson had predicted that if the two superconductors separated by a thin insulating barrier were current biased with a frequency f, the junction would develop a region of constant voltage steps at the values $nhf/2e$, where n is an integer. Shapiro verified the prediction experimentally in 1963 [Shapiro 1963]. If the ac current applied to the junction is within a certain range it will cause the flux quanta passing through the junction to phase lock to the applied frequency. With this phase lock the voltage across the junction is precisely $hf/2e$, and is known as the *ac Josephson* effect [Benz & Hamilton 2004]. Phase lock can also occur at various harmonics of the Josephson effect. This precise voltage is independent of the junction quality and can be used for a voltage standard. In the early 1970s many laboratories began assigning a value to the Josephson constant $K_J = 2e/h$ and using it as a voltage standard [Benz and Hamilton 2004], By international agreement in 1990 the constant $K_{J\text{-}90}$ was assigned the value 483,597.9GHz/V and adopted by all standards laboratories [Quinn 1989]. Because frequencies can be measured with extremely high accuracy the voltage defined by the Josephson constant improved the accuracy of the standard volt by orders of magnitude. Instead of relying on a chemical cell that had to be transported for voltage comparisons, laboratories anywhere in the world could fabricate a Josephson junction and use it to obtain the same voltage steps as anyone else. Typically the total uncertainty of a measurement using the Josephson effect is a few nanovolts. Many commercial instrument manufacturers now rely on a commercially available Josephson junction voltage standard in which liquid helium is used to maintain the Nb junctions in the superconducting state. Junction fabrication has advanced to the point where arrays of thousands of junctions have variations of critical current and resistance of only a few percent. Such arrays can then be used to provide a voltage standard at higher voltage values and to even program any desired precise output voltage up to 10 V from dc to 100 Hz [Benz and Hamilton 2004].

Josephson junctions are being used as detectors and mixers of low-level, high frequency signals from a variety of sources. They provide enhanced resolution for millimeter and submillimeter astrophysics signals [Zmuidzinas and Richards 2004]. When a SQUID is used to detect small changes in resistance of a superconducting film at a temperature in the transition region between the normal and superconducting states, the detector is known as a transition-edge sensor (TES detector). Such detectors typically operate at a temperature near 100 mK where the material specific heat is extremely low. Thus, very small power inputs will cause relatively rapid and large temperature changes in the detector (known as a bolometer) and result in a resistance change detected by the SQUID. When these devices are used to detect integrated energies they are known as microcalorimeters. They are very sensitive to low energy X-rays and can be used for X-ray astronomy [White and Tananbaum 1999] or for X-ray spectroscopic microanalysis of semiconductors [Wollman et al 1999]. Large arrays of TES detectors amplified with multiplexed SQUID arrays are now used for a variety of astronomical studies. **Figure 25a** shows a 10,240 pixel TES array amplified with a 5120 pixel SQUID amplifier array (**Figure 25b**), both developed at NIST for used on the SCUBA-2 submillimeter telescope in Hawaii. The TES array is cooled to about 100 mK with an adiabatic demagnetization refrigerator, which in turn is precooled to 4 K with a pulse tube cryocooler.

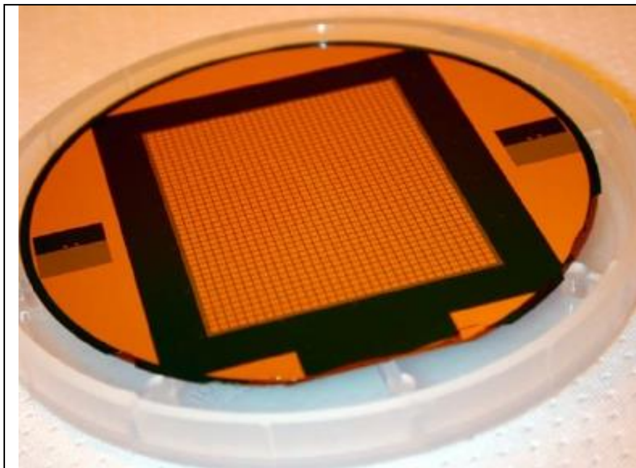	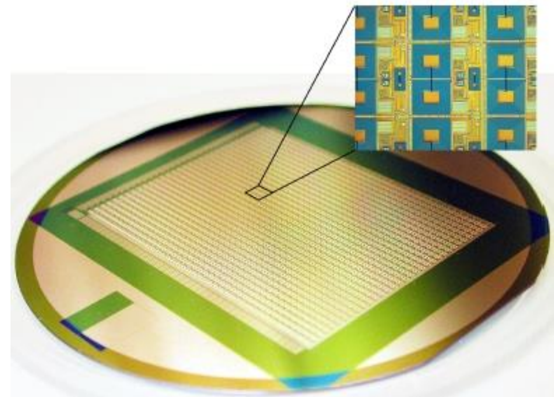
Figure 25a: Transition edge sensor (TES) array for the SCUBA-2 submillimeter telescope. NIST photo	**Figure 25b**: SQUID current amplifier array with 10,240 pixels for amplifying signals from the TES array shown on left. NIST photo

A superconducting film can be made to switch from the superconducting state to the normal state by applying a magnetic field from a nearby control line. Such a switch, known as a cryotron, can be used for digital electronics and was first studied in 1956 by Buck [Buck 1956]. The switching was quite slow because it relied on a thermal effect [Hayakawa et al 2004]. After the development of the Josephson junction devices various binary switching mechanisms were studied that made use of the Josephson junction and were much faster than the original cryotron. During the period of 1983 to 1987 various high-speed switching mechanisms using single flux quanta (SFQ) were investigated [Hayakawa et al 2004]. Then in 1987 a very high speed logic system emerged that was called rapid SFQ (RSFQ) [Mukhanov et al 1987] that could be operated at frequencies up to 100 GHz or higher. Such superconducting digital electronic systems have been developed worldwide for logic systems [Hayakawa et al 2004]. The use of SFQ logic for the following applications has been investigated: digital signal processing for digital filtering and multiuser detectors, digital sensor readout, switches for routers, and high end computing. High-end computing studies are focusing on a goal of 1 exaflops (10^{18} floating point operations per second) by 2020. Weather modeling over a two-week time span may require zettaflops (10^{21} flops). The K-computer in Japan with a speed of 10 petaflops (10^{16} flops) uses semiconductor circuits which require about 1 nJ per operation. A simple scaling to 1 exaflops indicates a power demand of 1 GW for each computer of that speed. With RSFQ logic, the switching energy is only about 10^{-19} J. Recent developments showed that the DC bias resistors with their relatively high power dissipation could be eliminated [Herr 2011 and Mukhanov 2011].

In 2005 the National Security Agency (NSA) convened a panel of experts to investigate the use of RSFQ logic for petaflops-scale high end computing at speeds not possible with semiconductor logic. The study recommended the development of a processor with approximately one million gates operating at a 50 GHz clock rate [National Security Agency August 2005]. A computer or processor of this complexity will require about one million Josephson junctions per chip with about ten chips. In order to keep time-of-flight short between various parts of the processor the processor needs to be kept rather small, on the order of a cubic meter, and with very careful architecture to achieve that clock speed. Niobium technology would be used for the Josephson junctions.

A major application of superconducting electronics that does not involve Josephson junctions is the superconducting microwave filter systems for cellular telephone base stations. They use HTS microstrip designs fabricated on wafer substrates. Because no junctions are involved HTS material provides very good performance with low noise. The most common substrate material to date has been MgO [Simon et al 2004]. Both YBCO and TBCCO have been used for the HTS material. **Figure 26** shows two common geometries used for the superconducting film in the filter. **Figure 27** compares the insertion loss versus the frequency for the superconducting filter (solid line) compared with a conventional filter. **Figure 28** shows the complete system in the form of a rack mounted unit. The filter system is cooled to about 77 K with a Stirling cryocooler that incorporates gas bearings to support the piston in the cylinder with no contact between the piston and cylinder walls. Refrigeration power of the Stirling cryocooler is about 6 W at 77 K with 100 W of input electrical power. **Figure 29** shows the rapid increase in the number of superconducting filter systems that have been deployed since 1998 when the first units were sold. Over 4000 are now in use, which has exceeded 1 % of the total number of base station filter systems.

Figure 26a: Geometry of SISO resonator.

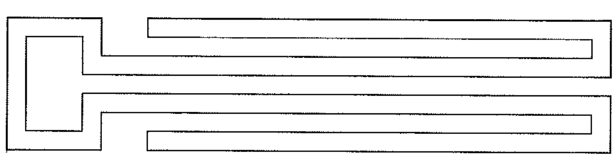

Figure 26b: Geometry of clip resonator for HTS microwave filters.

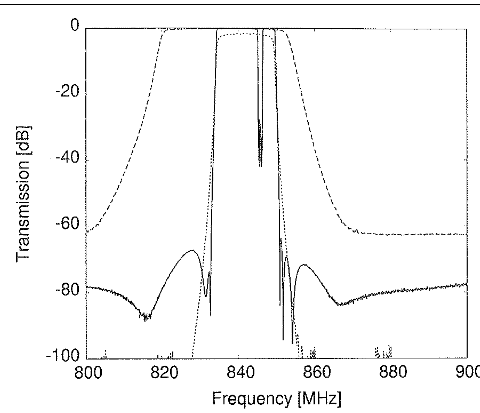

Figure 27: Insertion loss for three base station filters: dashed line, normal filter; solid line, HTS filter. (Simon et al 2004)

15.3.3.3 Applications of Superfluidity

When liquid ^{4}He is cooled below 2.17 K at atmospheric pressure, it undergoes a phase transition to a superfluid state known as helium II. In contrast, normal liquid helium is referred to as helium I. The phase transition temperature is called the lambda point. Superfluid helium is a result of macroscopic quantum phenomena in which a portion of the fluid in the two-fluid model has "condensed" into the quantum mechanical ground state and makes no contribution to the entropy. In the superfluid state the wave functions of each atom overlap and cause the atoms to act in unison as though they were one particle. Atoms acting in unison do not collide with each other and have no friction. The superfluid portion increases as the temperature is lowered below the lambda point. This portion of the fluid has zero viscosity and can flow through molecular-sized pores with no friction. If a vessel containing superfluid helium is kept below the lambda point, a thin superfluid film about 30 nm thick will creep up an over the wall and drip off the bottom of the container like a self-starting siphon. The zero viscosity of the superfluid portion also gives helium II and extremely high effective thermal conductivity brought about by the ease at which the superfluid can flow to the location of any heat input to absorb the heat. The thermal conductivity can approach infinity under ideal low heat flow conditions and hundreds of times that of copper in practical conditions. The high thermal conductivity causes the helium to evaporate at the saturation point without boiling. The lack of boiling is sometimes useful where vibration from boiling can interfere with sensitive experiments. The third unique and useful feature of superfluid helium is its very high specific heat, especially near the lambda point where considerable heat is required to change the superfluid portion to normal fluid. The specific heat can be as high as 10^5 times that of superconductors.

The three unique properties of superfluid helium mentioned above (zero viscosity, high thermal conductivity, and high specific heat) make it very useful for cooling superconducting magnets. First, the lower temperature of helium II coolant causes the critical magnetic field of a superconductor to increase. Then the zero viscosity of superfluid helium makes it easy to circulate it through the windings of a superconducting magnet to keep it cold. The high thermal conductivity of superfluid helium allows it to conduct heat long distances in regions of stagnant flow. The high specific heat allows it to act as a good stabilizer to prevent quenching of superconducting magnets in which a local disturbance in the superconductor leads to a propagating hot spot that drives the superconductor into the normal state.

As discussed in section 15.3.3.1, the 8.36 T magnetic field required of the dipole magnets in the Large Hadron Collider (LHC) at CERN was achieved by cooling the NbTi superconductor windings to 1.9 K with superfluid helium. The total refrigeration power at 1.9 K for all eight stations in the LHC is about 18 kW. Several earlier accelerators also used superfluid helium in the range of 1.8 to 1.9 K, but refrigeration powers were much lower. The acceleration of electrons in the Continuous Electron Beam Acceleration Facility (CEBAF) at Jefferson Lab makes use of 338 radio frequency (rf) cavities made with superconducting niobium [Delayen 1998]. The recent upgrade from 6 GeV to 12 Gev makes use of additional superconducting cavities. All are cooled to 2 K with superfluid helium for enhanced heat transfer and reduced rf losses in the niobium. The energy lost to heat in a niobium cavity is about 10^5 times smaller than in a copper cavity. Even so, 20 MW of input power is required to provide the 2 K cooling for the cavities and the 4.5 K cooling for superconducting bending magnets. A large variety of superconducting rf cavities are being used in particle accelerators because of the improved beam quality and high duty factor that they provide.

The zero entropy of the superfluid fraction in the two-fluid model of superfluid helium is a key to the operation of the ^{3}He-^{4}He dilution refrigerator, which can provide refrigeration down to about 2 mK. The superfluid fraction is close to one for temperatures below 1 K. When ^{3}He is added to superfluid ^{4}He, the thermodynamic properties of the mixture are dominated by that of the dissolved ^{3}He. The zero entropy of the ^{4}He component makes it act like a vacuum and simply separate the ^{3}He atoms as though they were a dilute gas. The enthalpy and entropy of the dilute ^{3}He is then higher than that of pure ^{3}He. The maximum solubility of ^{3}He in ^{4}He is about

6.4 mol% at temperatures less than about 0.1 K [Radebaugh 1967]. Any additional ^{3}He phase separates and floats on top of the dilute mixture as nearly pure ^{3}He. The dilute and pure ^{3}He are in equilibrium with each other, analogous to that of a gas and liquid. When ^{3}He is removed from the dilute phase, more ^{3}He from the concentrated phase enters the dilute phase to maintain the saturated ^{3}He concentration of 6.4 %. In the dilution process the increased enthalpy of the ^{3}He causes it to absorb heat. This process takes place in the mixing chamber of a dilution refrigerator. Separation of the ^{3}He from the dilute phase takes place in a still at a higher temperature of about 0.7 K where the vapor pressure of the dilute ^{3}He is high enough to be pumped away easily with a vacuum pump. The vapor pressure of ^{4}He at this temperature is much lower, so the gas phase has only 1 or 2 % of ^{4}He. The ^{4}He component is then stationary in the dilution refrigerator. The ^{3}He then diffuses through the superfluid ^{4}He in the tube connecting the still with the mixing chamber. In practice the tube is one side of a heat exchanger with the incoming pure ^{3}He. A room-temperature vacuum pump circulates the nearly pure ^{3}He.

15.3.4 Reduced thermal noise

The temperature of any object determines the thermal fluctuations of the atoms and electrons. Such fluctuations will lead to Johnson electrical noise if the device is part of an electrical circuit. The thermal noise power can be given by $P = 4kT\Delta f$, where k is Boltzmann's constant and Δf is the bandwidth. The voltage fluctuations across a resistor R become $V_n = (4kTR\Delta f)^{1/2}$. This noise voltage is reduced by cooling the resistor. Thus, in low noise applications it may be desirable to cool low noise amplifiers (LNA). In fact, the microwave filter systems discussed in the previous section also make use of cryogenically cooled low-noise amplifiers to keep system noise as low as possible.

Another form of noise is thermally radiated noise. The power associated with such radiation is proportional to temperature to the fourth power. Thus temperature reduction has a very pronounced effect on reducing radiated power. The temperature of an object also influences the intensity of the radiation. The wavelength at which the intensity is a maximum becomes greater with decreasing temperature. This wavelength is given by Wien's displacement formula,

$$\lambda_{max}T = 2.898 \text{ x } 10^{-3} \text{ K}\cdot\text{m}.$$

At 300 K, λ_{max} = 9.66 μm, whereas at 30 K the maximum occurs at 96.6 μm. These wavelengths are in the main part of the infrared spectrum which spans the range from about 0.7 μm to 1000 μm. For the detection of thermal radiation, the detector must be much colder than the object to be detected for the best sensitivity. Night vision equipment relies on detecting the thermally radiated electromagnetic spectrum. For military applications where high detectivity is desired to obtain good images of objects with small temperature variations, the infrared sensors or focal plane arrays are usually cooled to about 80 K for observation of objects near 300 K. The Stirling cryocoolers shown in chapter 6 are typical of what is used by the military for this application. Over 140,000 such coolers have been made since the early 1970s [Dunmire 1998]. There have been some limited spinoffs of this cooled infrared sensor technology to other areas, such as for police and rescue operations, security, and for process monitoring. In process monitoring small temperature changes in a product outside what is normal can be observed immediately, which allows the process to be modified or corrected in some way before a large inventory of unsatisfactory products accumulate.

Space applications of cooled infrared sensors are for either Earth observations or for astronomy observations. In civilian Earth observations the applications are for detection of small temperature changes in the atmosphere for aid in long range weather forecasting, for studies of the greenhouse effect and global warming, and for studies of the ozone hole. For military applications the need is for night vision of objects of interest. The military is also interested in observing objects that may be in space or heading out into space. If they are not being propelled by a rocket at that point in time, the sensors must be cold to observe the object that could be at 300 K or below. For astronomy most of the missions for the next 10 to 20 years will be for the study of the long wavelength infrared spectrum. There is much interest in the infrared wavelengths because (1) much of the universe is cold (planets), (2) there are regions that obscure other wavelengths, (3) dust in the universe is cold and can be studied in the infrared, (4) chemical compositions can be determined from molecular spectral lines that are common in the infrared, and (5) primordial light from the early Universe is highly redshifted due to cosmic expansion, in fact, only a small portion of the mass in the Universe can be observed in the visible wavelengths. The need for very efficient, lightweight, and reliable cryocoolers for this application has had a dramatic impact on improvements to cryocoolers over the past 20 years. Some of these improvements have found their way into the commercial marketplace, which have helped in other applications of cryogenics. Further details on these space-qualified cryocoolers are given by R. Ross elsewhere in this publication.

15.3.5 Low vapor pressures (cryopumping)

Figure 28 shows that vapor pressure of fluids decreases very fast as the temperature is lowered. For a surface at about 150 K the vapor pressure of water is reduced to 10^{-9} torr ($\approx 10^{-7}$ Pa). At 15 K even air or oxygen has a vapor pressure too small to be shown on the graph of **Figure 28**. Gases such as hydrogen, which may be outgassing products from semiconductor processing still have a high vapor pressure at 15 K. Its vapor pressure and that of helium can be greatly reduced at 15 K by the use of adsorption on a material with very high surface area, such as charcoal. The first atomic layer adsorbed on a surface has a pressure much below that of the normal vapor pressure. The vapor pressure curves for helium and hydrogen in equilibrium with an adsorbed monolayer are similar to those shown in **Figure** 28, except they are shifted to higher temperature by about an order of magnitude. The shift for other fluids decreases as the temperature is increased. For water, there is little difference compared with the vapor pressure curve shown in **Figure** 28.

Cryopumps, as shown in **Figure 29**, typically have a quantity of charcoal cooled to 15 K with the second stage of a Gifford-McMahon cryocooler to pump hydrogen and helium, and baffles cooled to about 60 K to cryopump most of the other gases to keep them from overloading the charcoal. This technique to produce high vacuum results in the ultimate cleanliness of the vacuum space, which is highly desirable for the semiconductor processing industry; especially as line spacing becomes less and less and any contaminant could short circuit the lines. The semiconductor processing industry has been the major user of such cryopumps. During the peak periods in semiconductor processing, about 20,000 cryopumps/yr were being sold. Within the last 10 years, another cryopumping procedure has become of some interest; wherein a dry turbo vacuum pump is used to pump most gases except water. The water is then cryopumped at very high speed with baffles cooled to about 110-120 K to assist the turbopump.

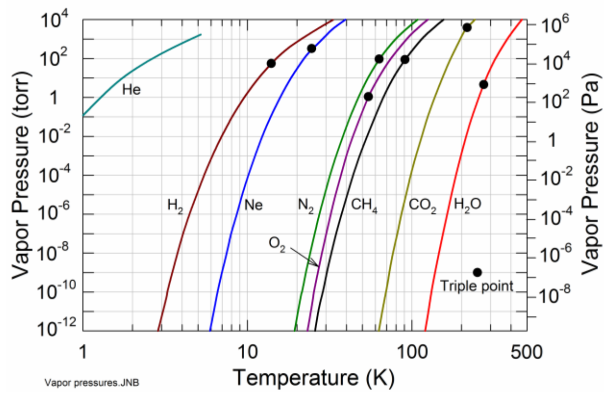

Figure 28: Vapor pressures of various gases at low temperatures. [IUVSTA, 2015]

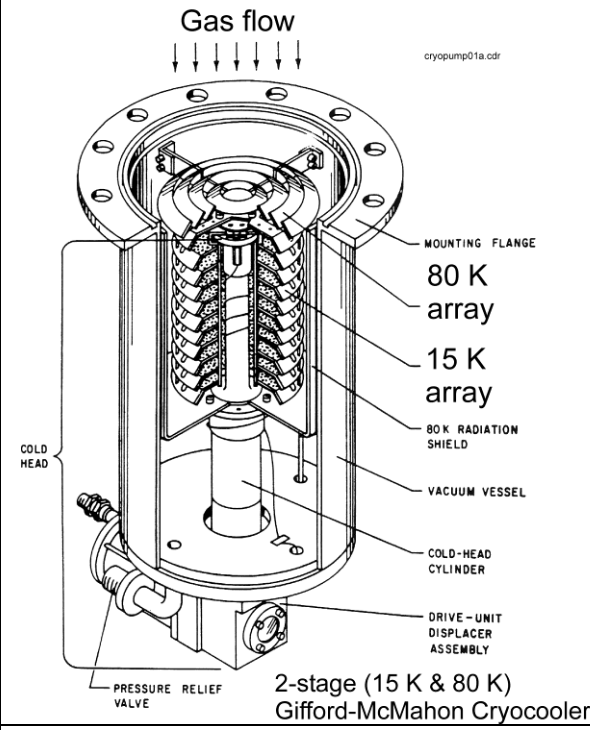

Figure 29: Cutaway drawing of a cryopump cooled with a Gifford-McMahon cryocooler. Courtesy Helix Technologies

15.3.6 Property changes (temporary or permanent)

Reducing the temperature of any material will always change its properties to some extent. Some materials undergo large property changes that can be useful for some applications. For example, the electrical resistivity of pure metals, such as copper or aluminum, decreases by several orders of magnitude when cooled from 300 K to 4 K. For commercially pure copper, such as grade 101 the change is about a factor of 100. Such a reduction in resistance can be useful in creating a high magnetic field without using superconducting wires. This change in resistivity of a metal is a temporary change, and the resistivity will revert back to the original value after the material is warmed back to the starting temperature.

A significant commercial application of cryogenics relies on the transition to a brittle glassy state of certain soft materials. The two primary examples are rubber and spices. At room temperature these soft materials are difficult to grind and require large amounts of energy. The recycling of rubber tires is accomplished by grinding the tire into small particles about 10 mm in diameter or smaller. Often a fine powder is desired for some applications, and with cryogenic grinding powder sizes down to 50 to 300 μm are possible since the energy required is greatly reduced. There is also less dust generated in the cryogrinding process compared to room temperature grinding. For safety reasons, a new tire contains less than 10 to 15% of recycled rubber. Thus, recycled tires are used mostly in other applications, such as various surfacing materials. Currently, about 13% of scrap tires in the US are recycled with about 1% being done cryogenically (Shatten 2004). One interesting approach now being investigated is the exploitation of the ‘free’ cold available at liquefied natural gas (LNG) regasification terminals to reduce the total energy required for cryogenic grinding [Shatten 2004; Shatten et al 2003].

Another cryogrinding application is that for spices and herbal medicines. India is the world’s largest grower and consumer of spices with an annual output of more than two million tons [Jacob et al 2000]. In conventional grinding of spices about 99 % of the applied energy gets dissipated in the form of heat; temperatures of 363 K have even been reported in some conventional grinding at high speeds [Pesek et al 1985]. This heating of the spices causes them to lose much of their highly volatile components, such as those contributing to aroma, and as a result their value suffers. Conversely, cryogrinding prevents overheating, which prevents a loss of oils and moisture. Throughput in a cryogenic grinding pilot plant was increased by a factor of 2.25 compared to ambient grinding [Jacob et al 2000]. In the cryogrinding of Chinese herbal medicines, one study found that about 1-5 kg of liquid nitrogen were used per kilogram of ground material [Li et al 1991].

A search on the web under cryogenics brings up many topics and company web sites dealing with cryogenic treatment of metals and other materials. This appears to have become a rather large business, impacting much of the general public with examples such as cryotreated razor blades, automobile parts, and machine tools; affording them all extended wear life. Scientific studies have shown that proper cryogenic treatment (slow cooling to liquid nitrogen temperature over a period of a day or more followed by a soak period of a day or so and slow warming can impart increased wear life to certain tool steels. A recent study in India [Lal et al 2001] and an earlier study by Barron [Barron 1982] describe the process and the effect on improved wear life in tool steels. Increased wear life of 2 to 6 times have been reported. These articles point out the importance of proper heat treatment prior to the cryotreatment. In essence the lower temperature brings about a more complete transformation of the austenitic microstructure to the harder martensitic phase. Though hardness of the metal does not change much, its wear life is significantly increased. This effect is being recognized by more manufacturers and is being adopted in a wide variety of applications. This is a permanent effect and requires only one treatment. Further research in this area is needed to better understand the effects and to determine the limitations.

15.3.7 Tissue ablation (cryosurgery)

Catheters with diameters of 3 mm or smaller are capable of accessing many internal organs through arteries and veins. They provide the medical community with tools to operate on internal organs without the need to cut through the body to gain access. As a result the use of catheters greatly speeds recovery times, reduces costs, and often reduces risks. The removal of unwanted tissue, such as cancer tumors or malfunctioning tissue can be carried out through cryoablation with cryogenic catheters. The effectiveness of these catheters depends very much on enhanced heat transfer at the very small tip. The recent development of small diameter and flexible cryogenic catheters has opened up the possibility of treating many abnormalities, including cancer, in internal organs without major surgery to gain access to the organ or to remove the organ. Instead of a several-day hospital stay and about a 6-week recovery period, the cryosurgical procedure can usually be performed as an outpatient service with local anesthesia that has a one-day recovery period.

Cryosurgery had its beginnings in 1851 when James Arnott used iced saline solutions to treat carcinomas of the breast and cervix [Arnott 1851; Fraser 1979]. The minimum temperature of –21 °C achievable with this technique is just at the upper limit for cell destruction [Dobak

1998] so Arnott had little success in curing the cancers, but achieved some beneficial effects, such as pain relief and reduction of bleeding. The use of solid carbon dioxide and liquid nitrogen around 1900 for cryosurgery [Le Pivert 1984] permitted much lower temperatures and more complete tissue destruction. These lower temperatures were commonly used in dermatological applications after 1900, but were not used much for deep-seated malignancies. One exception was the work of the neurosurgeon Temple Fay between 1936 and 1940 [Fay 1959]. He used implanted metal capsules connected to an external refrigeration system to treat brain tumors. He also used refrigerated liquids to treat large inoperable cancers of the cervix and breast. Few advances in cryosurgery followed until in 1961 the New York neurosurgeon Dr. Irving Cooper designed and used a cryosurgical probe cooled with liquid nitrogen to treat Parkinson's disease [Cooper and Lee 1961]. This event is often taken as the beginning of modern cryosurgery, although subsequent developments in medication have gone on to replace the cryosurgical approach for this disease.

In the mid-1960s Gonder and colleagues developed a modified liquid nitrogen cryosurgical systems for prostate cryosurgery [Gonder et al 1964]. Extensive animal experiments were carried out that lead to a broader clinical use of cryosurgery. Up to that point liquid nitrogen was the most common cryogen used in cryosurgery, but it had certain disadvantages. It could not be stored for long periods of time and it required bulky supporting equipment. Thus, the equipment could not be easily moved from room to room, and was not easy to use or control. The freezing process could not be stopped quickly because of the time for the liquid to drain from the probe. Vacuum insulated probes were required to prevent freezing along the length of the probe. Many advances in cryosurgical probes have occurred since 1961, and a much better understanding of tissue destruction at cold temperatures has developed. Advances in cryobiology have shown that cell temperatures of –40 °C or lower result in complete destruction of cancerous tissue, though somewhat higher temperatures up to about –20 °C may lead to destruction of some healthy tissue [Gage 1979; Gage 1992]. It has also been found that the lethal cell temperature can be increased by repeated freeze/thaw cycles and by rapid cooling and slow warming [Dobak 1998]. In the last 40 years several cooling methods have been developed and used for cryogenic catheters and probes. It was during this period that Joule-Thomson (JT) systems with high-pressure argon and nitrous oxide (N_2O) were introduced. Expansion of these fluids from high to low pressure results in cooling and liquefaction of the fluid. Liquid argon (-186 °C), liquid nitrous oxide (N_2O) (-88 °C), and various hydroflourocarbons (HFCs) and fluorocarbons (FCs) (-30 °C to –80 °C) are now used as refrigerants in addition to liquid nitrogen (-196 °C). Mixtures of pure fluids have recently been used [Marquardt et al 1998; Missimer 1994; Radebaugh 1996] that allow for a wide range of boiling temperatures between –30 °C and –196 °C.

The 1980s saw the development of a competing technology, that of electrosurgical or radio frequency (rf) catheters that destroy tissue by heating them to temperatures above about 42 °C. These rf catheters are simpler and easy to control. However, they are limited to the amount of tissue they can destroy at one location because the temperature difference between the 42 °C destruction temperature and the catheter tip is limited by the 100 °C boiling point of the water in the tissue. The rf catheters have been widely accepted by the medical community for the past three decades. The later development of cryogenic catheters has hindered their use in place of the rf catheters.

Beginning in the 1990s the development of improved cryosurgical probes along with advances in ultrasound and MRI imaging to locate the ice front have resulted in considerable interest within the medical community in the use of cryosurgery for a variety of applications

[Rubinsky 2000]. Early applications were mostly for treatment of abnormalities near the body surface. However, the recent development of small diameter and flexible cryogenic catheters has opened up the possibility of treating many abnormalities, including cancer, in internal organs without major surgery to gain access to the organ or to remove the organ. Instead of a several-day hospital stay and about a 6-week recovery period, the cryosurgical procedure can usually be performed as an outpatient service with local anesthesia that has a one-day recovery period. For example, a new cryogenic catheter [Dobak et al 2000] received the approval by the U.S. Food and Drug Administration (FDA) in 2001 to treat women with abnormal menstrual bleeding by freezing the uterine lining instead of surgically removing the uterus in a hysterectomy [Parker-Pope 2001]. Another new cryogenic catheter has been developed for the treatment of cardiac arrhythmias, or irregular heart beating [Ryba 2001]. Over 5 million people in the world's developed countries suffer from some form of heart arrhythmia. Current treatments involve medication or the use of rf catheters. Heart arrhythmia occurs when a portion of the heart distorts its electrical signals. Ablating the tissue that distorts these electrical signals with either rf or cryogenic catheters eliminates the arrhythmia in almost all cases. Though newer than rf catheters, the cryogenic cardiac catheters offer the following advantages: (1) cryomapping capability, (2) not susceptible to forming blood clots, and (3) will stick to the tissue once freezing begins and not be moved out of place by heart movement. The cryogenic cardiac catheters are one of the most challenging cryogenic catheters in terms of refrigeration and heat transfer issues. The catheter is about 3 mm in diameter and about 1 m long. It is inserted through a small incision into a large vein in the leg in the groin area. For treatment of atrial fibrillation, it enters the right atrium of the heart via this vein and continues into the left atrium through a hole punctured previously in the wall between the two chambers. As shown in **Figure 30**, the catheter tip is placed at the junction to the pulmonary vein coming from the lungs, at which time a small balloon is inflated at the tip to temporarily block the blood flow. Finally, refrigerant flow into the balloon is initiated to cause freezing of the necessary tissue around the perimeter of the junction. Recent reviews of the procedure show it to be as successful as rf catheters with some advantages and improved safety [Ozcon et al. 2011].

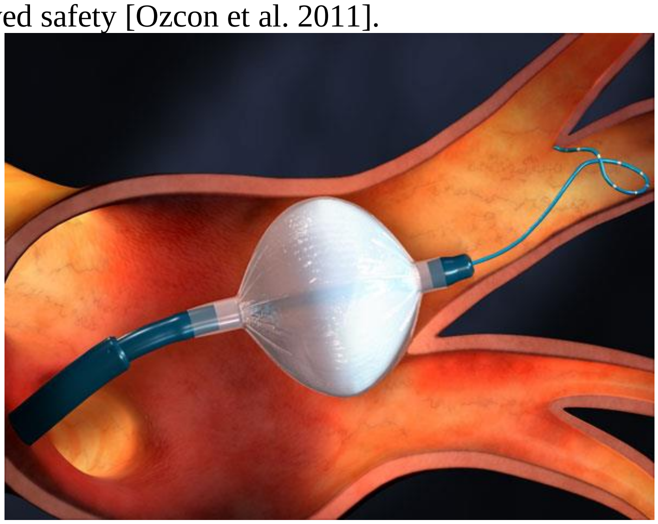

Figure 30: Cryoballoon catheter for the treatment of atrial fibrillation shown in place at the junction to the pulmonary vein. N_2O refrigerant is then flowed into the balloon for about 5 minutes to perform the ablation. Courtesy Medtronics

Further improvements in cryosurgical probes could open up many more medical applications, including the treatment of cancers of the liver, breast, and lung. Successful application of cryosurgical probes is very much dependent on providing a well-controlled cooling rate at the tip with little or no cooling along the length of the probe. To reach further into the body, catheters need to be made smaller and smaller. Large amounts of heat (often 10s of watts) need to be removed at the catheter tip in order to freeze a large-enough region at a sufficiently fast rate to provide well-defined regions of tissue destruction. Cryosurgery applications have the potential to expand considerably and become a major medical procedure if the following developments occur: (a) the medical device community has the information needed to help them select the optimum cooling method in a cryosurgical probe for a particular application, (b) a given heat removal rate can be achieved in smaller and smaller cryogenic catheters, and (c) compact, reliable, and-easy-to-use catheter systems are readily available that can be applied to various procedures. Recent reviews of cryosurgery have been given by [Dobak 1998; Rubinsky 2000; Theodorescu 2004; Gage et al 2009]

15.4 Challenges to the Use of Cryogenic Temperatures

Cryogenic temperatures can provide many benefits, but any particular application will not be commercially successful if the challenges of reaching such temperatures become too great. The use of liquid cryogens has been a common practice in many applications, but the need to periodically replenish the cryogen can become a challenge and ultimately hinder the use of cryogenic temperatures. This is especially true with the case of liquid helium as the price of helium is increasing rapidly and its availability is limited. The use of liquid cryogens is being replaced in many applications with the use of closed-cycle refrigeration systems or cryocoolers [Chapter 6]. However, cryocoolers have their own disadvantages that often present challenges in adapting them for a particular application. These disadvantages were listed at the beginning of this chapter. Research on cryocoolers in the last 50 years has made great strides in minimizing these disadvantages. Space applications in particular have been a strong driver for increasing cryocooler lifetimes from a few hundred hours to as much as ten years. Space applications have also led to significantly increased efficiencies and reduced sizes of cryocoolers, and commercial applications have been a strong driver to reduce costs. The ultimate goal for all of cryogenic applications is to hide the fact that cryogenic temperatures are needed to produce the benefit that it provides. In most cases the end user cares only about the benefits and doesn't want the cryogenics to be obvious in terms of problems, such as reliability, power, size, noise, cost, etc. Significant reductions of these disadvantages will inevitably lead to more applications. Many advances in cryocoolers have been made in the last 50 years that have had a major impact, and led to many applications of cryogenics that would not have been possible 50 years ago.

15.5 Summary/Conclusions

Operating at cold temperatures is essential to many fields of science and engineering including space exploration, electronics and medicine. One of the areas that require low temperature materials and mechanisms is related to planetary exploration of bodies in the solar system that are extremely cold. This includes potential NASA in-situ exploration missions to Europa and Titan where the ambient temperature is in the range of -200^{o}C. Generally, material properties change at low temperatures and these changes affect the strength, thermal conductivity, ductility, and electrical resistance.

With the increased availability of effective cooling mechanisms and the reduction in their cost, there is a growing interest in technologies that are applicable at low temperature. As a method of slowing or halting chemical and biological processes, cooling is widely used as a means of preserving food, chemicals, as well as biological tissues and organs. Further, as a method of reducing electrical conductivity cooling to produce superconductivity enables unique capabilities including levitation, highly efficient electromagnets, and others. The subject of low temperature materials and mechanisms is multidisciplinary and it involves various related science and engineering disciplines including chemistry, material science, electrical engineering, mechanical engineering, metallurgy, and physics.

Various methods are applied to reach cryogenic temperatures including the use of boiling cryogens, compression and expansion of gases, adiabatic demagnetization, and fluid mixing. The tools that allow reaching cryogenic temperatures are called cryocoolers and they are mostly based on heat exchange. Applications of cryogenic temperatures include such fields as physics, chemistry, materials science, and biology.

There are many challenges to producing and applying low temperatures and they significantly increase as the temperature drops. The challenges are continually being addressed as the number of applications grows.

15.6 Acknowledgement

Some of the research reported in this Chapter was conducted at the Jet Propulsion Laboratory (JPL), California Institute of Technology, under a contract with the National Aeronautics and Space Administration (NASA).

15.7 References

(DVB) SA. 2003. LNG Tanker Market Report, DVB Research & Strategic Planning, Rotterdam 101: 129-34

Anderson PW, Rowell JM. 1963. Probable observation of the Josephson superconducting tunnel effect. *Phys. Rev. Lett.* 10: 230

Andrews DE. 1988. Magnetic Resonance Imaging in 1987 In *Adv. Cryogenic Engineering*, pp. 1-7. New York: Plenum Press

Arnott J. 1851. *On the Treatment of Cancer through the Regulated Application of an Anaesthetic Temperature*.

Baker CR, fisher TF. 1992. Industrial cryogenic engineering in the USA In *History and Origins of Cryogenics*, ed. RG Scurlock, pp. 217-54. London: Clarendon Press

Bar-Cohen Y., "(Ed.), *High Temperature Materials and Mechanisms*, ISBN 13: 9781466566453, ISBN 10: 1466566450, CRC Press, Taylor & Francis Group, Boca Raton, Florida (March 2014) pp. 1-551

Bardeen J, Cooper LN, Schrieffer JR. 1957. Theory of Superconductivity. *Phys. Rev.* 108: 1175

Barron RF. 1982. Cryogenic treatment of metals to improve wear resistance. *Cryogenics* 22: 409-13

Bednorz JG, Muller KA. 1986. Possible High Tc Superconductivity in the Ba-La-Cu-O System. *Z. Phys. B - Condensed Matter* 64: 189193

Benz SP, Hamilton C. 2004. Application of the Josephson Effect to Voltage Metrology. *Proc. IEEE, Special Issue on Applications of Superconductivity* 92: 1617-29

Buck DA. 1956. The cryotron--A superconducting computer component. *Proc. IRE* 44: 482

Bunge RG, Sherman JK. 1953. Fertilizing capacity of frozen spermatoza. *Nature* 172: 767

Bureau USC. 2004. Industrial Gas Manufacturing: 2002*EC02-311-325120*, U.S. Census Bureau, Washington
Bureau USC. 2005. Industrial Gas Production, U.S. Census Bureau, Washington
Cantor R, Vinetskiy V, Matlashov A. 1996. A low noise, integrated dc SQUID magnetometerfor applications in biomagnetism In *Proc. Biomag. 96*, ed. YO C. J. Aine, G. Stroink, S. J. Swithenby, and C. C. Wood
CCAS 2015. Coalition for the Commercial Application of Superconductivity, http://www.ccas-web.org/superconductivity/medicalimaging/
Chen C. 1986. Pregnancy after human oocyte cryopreservation. *Lencet* 1: 884
CLNG 2015. Center for Liquefied Natural Gas, www.lngfacts.org
Cooper IS, Lee AS. 1961. Cryostatic Congelation: A System for Producing a Limited Controlled Region of Cooling or Freezing of Biological Tissues. *J. Nerv. Ment. Dis.* 133: 259-69
Corporation AS. 2005. Ship Propulsion.
Dai P, Chakoumakos BC, Sun GF, Wong KW, Xin Y, Lu DF. 1995. Synthesis and Neutron Powder Diffraction Study of the Superconductor HgBa2Ca2Cu3O8+ by Tl Substitution. *Physica C* 243: 201-06
Damadian R. 1977. NMR in cancer: XVI. Fonar image of the live human body. *Physiol. Chem. & Phys.* 9: 97-100
Damadian RV. 1971. Tumor detection by nuclear magnetic resonance. *Science* 171: 1151-53
Damadian RV. 1974. *US Patent No. 3,789,832*
Delayen JR. 1998. The Jefferson Lab Superconducting Accelerator, in *Adv. Cryogenic Engineering*, vol. 43, pp. 37-42, New York: Plenum Press
Delikaris D, Tavian L. 2014. *J. Cryo. Super. Soc. Jpn*. 49: 590-600
Devred A, Desportes H, Kircher F, Lesmond C, Meuris C, et al. 1998. Superconducting Magnet Technology In *Handbook of Cryogenic Engineering*, ed. JGW II, pp. 321-64. Philadelphia: Taylor & Francis
Dobak J, Ryba E, Kovalcheck S. 2000. A New Closed-Loop Cryosurgical Device for Endometrial Ablation. *J. Am. Assoc. Gynecol. Laparosc* 7: 245-49
Dobak J. 1998. A Review of Cryobiology and Cryosurgery In *Adv. Cryogenic Engineering*, pp. 889-96
DOE/EIA. 2014. Annual energy Outlook 2014, *DOE/EIA-0383 (2014)*, Department of Energy/Energy Information Administration, Washington
Drung D, Bechstein S, Franke K-P, Schreiner M, Schurig T. 2001. Improved direct-coupled DC SQUID read-out electronics with automatic bias voltage tuning. *IEEE Trans. Appl. Superconductivity* 11: 880-83
Drung D, Ludwig F, Muller W, Steinhoff U, Trahms L, et al. 1996. Integrated YBCO magnetometer for biomagnetic measurements. *Appl. Phys. Lett.* 68: 1421-23
Dunmire H. 1998. *U.S. Army cryocooler status update.* Presented at Second Workshop on Military and Commercial Applications for low Cost Cryocoolers (MCALCII), San Diego
Edwards HT. 1985. The tevatron energy doubler: A superconducting accelerator. *Annu. Rev. Nucl. Part. Sci.* 35: 605-60
EPA 2008. Technical Support Document for Hydrogen Production: Proposed Rule for Mandatory Reporting of Greenhouse Gases, U. S. Environmental Protection Agency, Office of Air and Radiation
Fay T. 1959. Early Experiences with Local and Generalized Refrigeration of the Human Brain. *J. Neurosurg.* 16: 239-59

Foote RH. 2001. The history of artificial insemination: Selected notes and notables. *Am. Soc. Animal Science* 2002: 1-10
Foote, R.H., "The history of artificial insemination: Selected notes and notables," *Am. Soc. Animal Science*, vol. 2002, (2001), pp. 1-10.
Fraser J. 1979. Cryogenic Techniques in Surgery. *Cryogenics* 19: 375-81
Freiman A, Bouganim N. 2005. History of Cryotherapy. *Dermatology Online Journal* 11: Article #9
Freiman A., and Bouganim, N., "History of Cryotherapy," *Dermatology Online Journal*, vol. 11, Article #9, 2005.
Gage AA, Baust JM, Baust JG. 2009, Experimental cryosurgery investigations in vivo. *Cryobiology* 59: 229-243.
Gage AA. 1979. What Temperature is Lethal for Cells. *J. Derm. Surg. Oncol.* 464: 459-60
Gage AA. 1992. Cryosurgery in The Treatment of Cancer. *Surgery, Gynecology, and Obstetrics* 174: 73-92
Global Industy Analyst 2015. http://www.prweb.com/releases/superconductors/super_conductors/prweb12176943.htm
Goldsmith M, Damadian R, Stanford M, Lipkowitz M. 1977. NMR in Cancer: XVIII. A Superconductive NMR Magnet for a Human Sample. *Physiol. Chem. & Phys.* 9: 105-07
Gonder M, Soannes W, Smith V. 1964. Experimental Prostate Cryosurgery. *Invest. Urol.* 1: 610-19
Gourlay SA, Sabbi G, Kircher F, Martovetsky N, Ketchen D. 2004. Superconducting Magnets and their Applications. *Proc. IEEE, Special Issue on Applications of Superconductivity* 92: 1675-87
Grenier M, Petit P. 1986. Cryogenic air separation: The last twenty years In *Adv. Cryogenic Engineering*, pp. 1063-70. New York: Plenum Press
Grossman HL, Meyers WR, Vreeland VJ, Bruehl R, Alper MD, et al. 2004. Detection of bacteria in suspension using a superconducting quantum interference device. *Proc. Nat. Acad. Sci.*
Haselden GG. 1992. The history of liquefied natural gas (LNG) In *History and Origins of Cryogenics*, ed. RG Scurlock, pp. 599-619. Oxford: Clarendon Press
Hayakawa H, Yoshikawa N, Yorozu S, Fujimaki A. 2004. Superconducting Digital Electronics. *Proc. IEEE, Special Issue on Applications of Superconductivity* 92: 1549-63
Herr QP. 2011 Ultra-low power superconducting logic, *J. Appl. Phys.*109: 103903.
Hulm JK, Blaugher RD. 1961. *Phys. Rev.* 123: 1569
IUVSTA. 2015. International Union for Vacuum Science, Technique, and Applications, http://www.iuvsta.org/iuvsta2/index.php?id=643
Jacob S, Kasthurirengan S, Karunanithi R, Behera U. 2000. Development of pilot plant for cryogrinding of spices: A method for quality improvement In *Adv. Cryogenic Engineering*, pp. 1731-38. New York: Plenum Publishers
Jaklevic RC, Lambe J, Silver AH, Mercereau JE. 1964. Quantum interference effects in Josephson tunneling. *Phys. Rev. Lett.* 12: 159-60
Josephson BD. 1962. Possible new effects in superconducting tunneling. *Phys. Lett.* 1: 251-53
Kalinine V, Haange R, Shatil N, Millet F, Jager B, et al. 2004. Design and operating features of the ITER 4.5 K cryoplant In *Adv. Cryogenic Engineering*, pp. 176-83: American institute of Physics

Kalsi SS, Weeber K, Takesue H, Lewis C, Neumueller HW, Blaugher RD. 2004. Development Status of Rotating Machines Employing Superconducting Field Windings. *Proc. IEEE, Special Issue on Applications of Superconductivity* 92: 1688-704

Kato T, Kubota M, Kobayashi N, Suzuoki Y. 2003. *Effective utilization of by-product oxygen of electrolysis hydrogen production.* Presented at International Energy Workshop, June 23-25, 2003

Kleiner R, Koelle D, Ludwid F, Clarke J. 2004. Superconducting quantum Interference Devices: State of the Art and Applications. *Proc. IEEE, Special Issue on Applications of Superconductivity* 92: 1534-48

Kumar A, Welti D, Ernst RR. 1975. NMR Fourier zeugmatography. *J. Magn. Res.* 18: 69-83

Kunzler JE, Buehler E, Hsu FSL, Wernick JH. 1961. *Phys. Rev. Lett.* 6: 89

Kuriyama T. 2003. Private communication. ed. R Radebaugh

Kuriyama T. 2005. Private communication. ed. R Radebaugh

Lal DM, Renganarayanan S, Kalanidhi A. 2001. Cryogenic treatment to augment wear resistance of tool and die steels. *Cryogenics* 41: 149-55

Lauterbur PC. 1973. Image formation by induced local interactions: examples employing nuclear magnetic resonance. *Nature* 242: 190-91

Le Pivert P. *10th International Cryogenic Engineerig Conf., Butterworth, Surrey, 1984*: 551-57.

Li S, Ge S, Huang Z, Wang Q, Zhao H, Pan H. 1991. Cryogenic grinding technology for traditional Chinese herbal medicine. *Cryogenics* 31: 136-37

Maeda H, Tanaka T, Fukutomi M, Asano T. 1988. *J. Appl. Phys.* 27: L209

Magnetic Resonance 2015, www.magnetic-resonance.org, chapter21-02

Malozemoff AP, Mannhart J, Scalapino D. 2005. High-Temperature Cuprate Superconductors Get to Work. *Phys. Today*: 41-47

Mansfield P, Maudsley AA. 1976. Planar spin imaging by NMR. *J. Phys. C: Solid State Phys.* 9: L409-11

Mansfield P. 1977. Multi-planar image formation using NMR spin-echos. *J. Phys. C: Solid State Physics* 10: L55-L58

Marquardt ED, Radebaugh R, Dobak JA. 1998. Cryogenic Catheter for Treating Heart Arrhythmia In *Adv. Cryogenic Engineering*, pp. 903-10

Marquardt ED, Radebaugh R. 2000. Pulse tube oxygen liquefier In *Adv. Cryogenic Engineering*, pp. 457-64. New York: Plenum Press

Matthias BT, Geballe TH, Geller S, Corenzwit E. 1954. Superconductivity of Nb3Sn. *Phys. Rev.* 95: 1435

Missimer DJ. *Tenth Intersociety Cryogenic Symposium (AIChE Spring National Meeting, March1994*.

Mukhanov O, Semenov V, Likharev K. 1987. Ultimate performance of the RSFQ logic circuits. *IEEE Trans. Magn.* vol. MAG-23: 759-62

Mukhanov O. 2011, Energy-Efficient Single Flux Quantum Technology, *IEEE Trans. Appl. Superconductivity* 21, 760-769.

Muller WH-G, Hopfel D. 1998. Magnetic resonance imaging and spectroscopy (medical applications) In *Handbook of Applied Superconductivity*, pp. 1213-48. Bristol: Institute of Physics Publishing

National Security Agency OoCA, www.nitrd.gov. August 2005. Supercondcuting Technology Assessment

Notardonato WU 2014. Development of a Ground Operations Demonstration Unit for Liquid Hydrogen at Kennedy Space Center, *25th International Cryogenic Engineering Conference and the International CryogenicMaterials Conference*, Elsevier B.V, Amsterdam, Netherlands.
ORNL 2005. Materials for separation technologies: energy and emission reduction opportunities, Department of Energy, Washington
Oshima K, Aiyama Y. 1992. The development of cryogenics in Japan In *History and Origins of Cryogenics*, ed. RG Scurlock, pp. 520-46. Oxford: Clarendon Press
Ozcan C, Ruskin J, Mansour M. 2011. Cryoballoon Catheter Ablation in Atrial Fibrillation. *Cardiology Research and Proactice* 2011: 256347.
Parker-Pope T. 2001. FDA Clears Devices that Help to Treat Difficult Menstruation. *The Wall Street Journal, Health Journal, May 4*:
Pesek CA, Wilson LA, Hammond EG. 1985. Spice quality: Effect of cryogenic and ambient grinding on volitiles. *J. Food Science* 50: 559
Quinn TJ. 1989. News from the BIPM. *Metrologia* 26: 69-74
Radebaugh R. 1967. Thermodynamic Properties of ^{3}He-^{4}He mixtures with Applications to the ^{3}He-^{4}He Dilution Refrigerator, NBS Tech. Note 362
Radebaugh R. *Proc. 19th International Congress of Refrigeration, The Hague, Netherlands, 1996*: 973-89.
Railway J. 2004. Overview of Maglev R&D. Railway Technical Research Institute, Japan Railway
Royal J. 2005. Private communication. ed. R Radebaugh
Rubinsky B. 2000. Cryosurgery. *Annual Review of Biomedical Engineering* 2: 157-87
Ryba E. 2001. Private communication. ed. R Radebaugh
Scanlan RM, Malozemoff AP, Larbalestier DC. 2004. Superconducting Materials for Large Scale Applications. *Proc. IEEE, Special Issue on Applications of Superconductivity* 92: 1639-54
Schilling DR. 2014. World's Largest Ship Ever Built and First Floating Liquefied Natural Gas (FLNG) Platform to Begin Drilling in 2017, Industry Tap, October 16, 2014.
Schwall RE. 1987. MRI--Superconductivity in the marketplace. *IEEE Trans. on Superconductivity* MAG-23: 1287-93
Scurlock, R.G., *History and Origins of Cryogenics*, Clarendon Press, Oxford (1992), pp. 28-29.
Shapiro S. 1963. Josephson currents in superconducting tunnelling: the effect of microwaves and other observations. *Phys. Rev. Lett.* 11: 80-82
Shatten, R.A. 2004. US patent issued for Super Cool's innovative energy conservation and cryogenic recycling method, in *Cold Facts (Cryogenic Society of America)*, vol. 20, Winter, pp. 34.
Shatten R.A., Carrier, J., and Jackson, J.D. 2003. System and method for cryogenic cooling using liquefied natural gas, US patent No. 6,668,562. USA
Shimomura Y. 2001. *Nuclear Fusion* 41: 309
Silver AH, Zimmerman JE. 1967. Quantum states and transitions in weakly connected superconducting rings. *Phys. Rev.* 157: 317-41
Simon RW, Hammond RB, Berkowitz SJ, Willemsen BA. 2004. Superconducting Microwave Filter Systems for Cellular Telephone Base Stations. *Proc. IEEE, Special Issue on Applications of Superconductivity* 92: 1585-96
Sloop JL. 1978. Liquid Hydrogen as a Propulsion Fuel, 1945-1959, NASA SP 4404

Theodorescu D. 2004. Cancer Cryotherapy: Evolution and Biology. *Reviews in Urology* 6, suppl. 4: S9-S19
Tishler AO. 1966. The impact of the space age on cryogenics In *Adv. Cryogenic Engineering*, pp. 1-10. New York: Plenum Press
Trill R. 2002. *Hydrogen as Alternative Fuel.* Presented at BMW Clean Energy Seminar, Sacramento, California
Trounson A, Mohr L. 1983. Human pregnancy following cryopreservation, thawing, and transfer of an eight cell embryo. *Nature* 305: 707
Week S. 2005. Edelstein, MRI pioneer, wins National Physics Prize. *Superconductor Week*, December 26, 2005:
White N, Tananbaum H. 1999. The constellation X-ray mission. *Astrophys. Lett. Comm.* 39: 933-36
Wollman DA, Hilton GC, Irwin KD, Bergren NF, Rudman DA, et al. 1999. Cryogenic microcalorimeters for X-ray microanalysis In *Proc. 1999 NCSL Workshop and Symp. (Nat. Conf. Standards Laboratories)*, pp. 811-19
World Steel 2014. World Steel in Figures, 2014 Edition, World Steel Association
Wu MK, Ashburn JR, Torng CJ, Hor PH, Meng RL, et al. 1987. *Phys. Rev. Lett.* 58: 908
Zmuidzinas J, Richards PL. 2004. Superconducting Detectors and Mixers for Millimeter and Submillimeter Astrophysics. *Proc. IEEE, Special Issue on Applications of Superconductivity* 92: 1597-616

15.7.1 Internet links

NIST Cryogenic Technologies Group – http://cryogenics.nist.gov
NIST Cryogenic Material Properties Database -
http://cryogenics.nist.gov/MPropsMAY/materialproperties.htm
Cryogenic Society of America, Cold Facts Newsletter, available from www.cryogenicsociety.org
Cryocooler - http://en.wikipedia.org/wiki/Cryocooler
Superconductivity - http://www.superconductors.org/Uses.htm ; http://www.superconductors.org/INdex.htm
www.eia.doe.gov.
www.tylermedicalclinic.com. 2005.